Book of Abstracts of the Workshop

Hydrodynamics at small scales: from soft matter to bioengineering

October 17-19, 2022
IISC, AR Auditorium
Bangalore (INDIA)

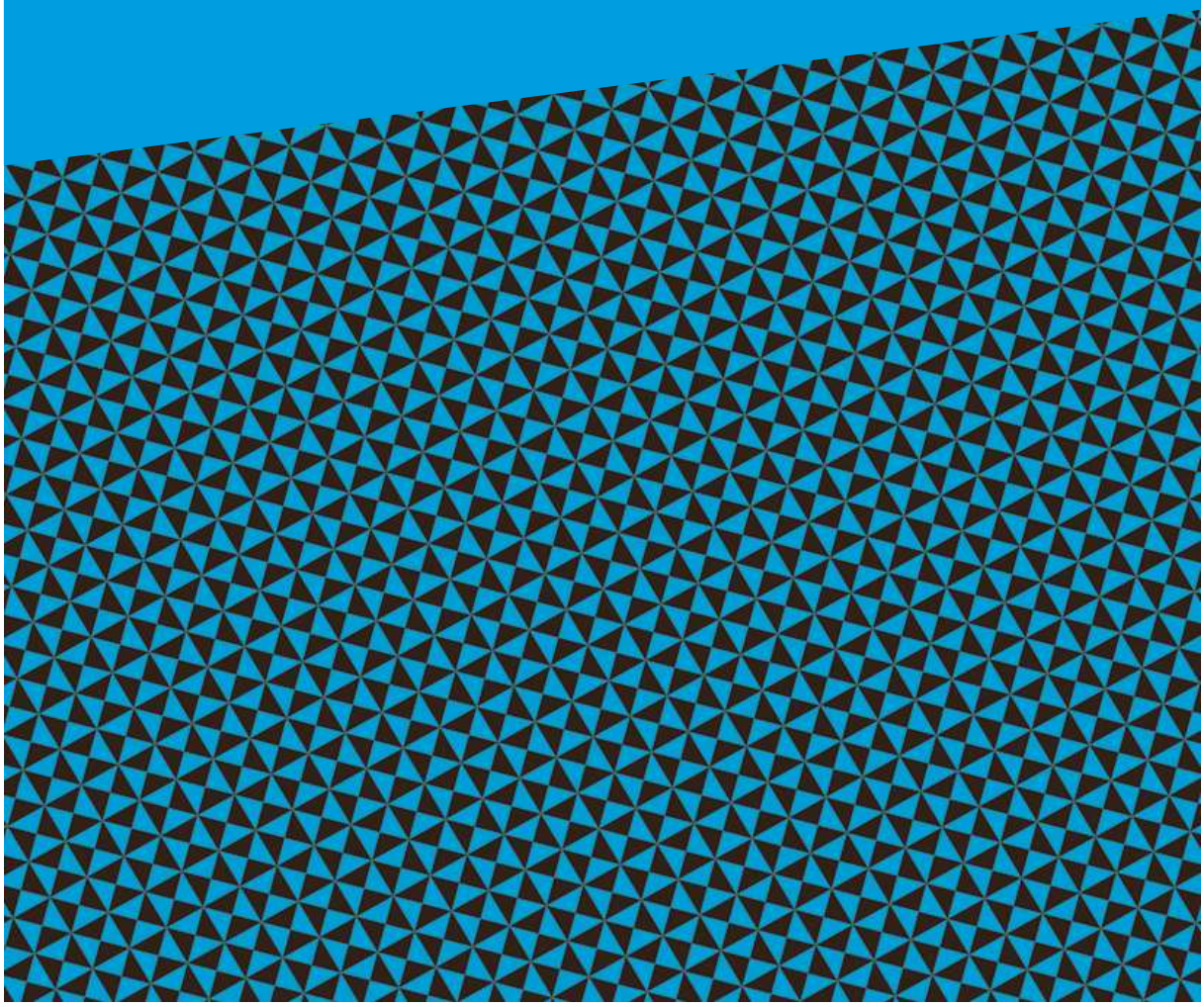

Table of contents

Microfluidic coflow systems exposed to bulk acoustic waves

Ashis Kumar Sen, E Hemachandran, and Sazid Zamal Hoque

Department of Mechanical Engineering, IIT Madras, 600036, Chennai, India ashis@iitm.ac.in

The transition between stream and droplet regimes in a coflow is typically achieved by adjusting the capillary numbers (Ca) of the phases. We experimentally evidence a reversible transition between the two regimes by controlling exposure of the system to acoustic standing waves, with Ca fixed. By satisfying the ratio of acoustic radiation force to the interfacial tension force, $\mathrm{Ca_{ac}} > 1$, experiments reveal a reversible stream-drop transition for $\mathrm{Ca} < 1$, and stream relocation for $\mathrm{Ca} \geq 1$. We explain the phenomenon in terms of the pinching, advection, and relocation timescales and a transition between convective and absolute instability from a linear stability analysis.

A continuous stream of a fluid in contact with another immiscible fluid can break into drops hallmarked by the Rayleigh-Plateau instability [1]. The instability is a direct consequence of the minimization of interfacial energy, related to interfacial tension and hydrodynamic force. In a confined system such as a microchannel, drops are typically produced using a flow-focusing or T-junction. Drop formation can occur either at the junction, as observed in squeezing and dripping regimes, or downstream at the end of a liquid jet, as in the jetting regime. While the dripping regime is a consequence of absolute instability, droplets in the jetting regime are produced through convective instability [2]. At higher Ca of the streams, growth of instability is suppressed as it gets entirely convected downstream resulting in the parallel flow regime, and droplets are not formed. The transition from the stream to the droplet regime and vice versa is typically achieved by adjusting the flow rate, consequently modifying the Ca of the phases [3]. However, the transition between the regimes achieved by altering the Ca inherits a longer time delay due to the response time of the fluidic system. One means of generating drops while operating at a higher and fixed Ca, and achieving a fast reversible transition between stream and droplet regimes would be to trigger the system with an external perturbation. Acoustic radiation force (ARF) due to standing bulk acoustic waves (BAW) can relocate coflowing immiscible streams and introduce perturbation [4]. The transition between stream and drop regimes by controlling the acoustic field will be advantageous as it does not require changing the Ca and therefore can offer a fast response time. This would be of significant scientific interest, and also of great value for technologies that require on-demand and fast transition between the stream and drop regimes, such as microfluidics, emulsification, and encapsulation. Despite great technological potential and scientific as well as industrial interest in droplet microfluidics, on-demand controlled generation of droplets at high Ca and reversible transition between the stream and drop regimes without altering the Ca is yet to be reported.

We study the reversible transition between stream and droplet regimes by exposing a coflow of immiscible liquids to a standing BAW, without altering the Ca of the two phases. Here, $\mathrm{Ca_i} = (\mu_i U_i/\gamma_{12})$, $i = 1,2$ respectively for streams 1 and 2. We use a microchannel device with a coflow system and identify the conditions for reversible transitions in terms of the Ca and acoustocapillary number $\mathrm{Ca_{ac}} = (E_{ac}\overline{\Delta Z}W/\gamma_{12})$, where E_{ac} is the acoustic energy density, $\overline{\Delta Z} = (Z_1 - Z_2)/Z_{avg}$ is the normalized acoustic impedance contrast, $Z_{avg} = (Z_1 + Z_2)/2$, Z_1 and Z_2 are respectively acoustic impedances of streams 1 and 2, and W is the channel width. When we exposed a coflow system of aqueous glycerol (80%) and mineral oil with $\Delta Z > 0$ and $\mathrm{Ca_{ac}} > 1$, for $\mathrm{Ca} < 1$, we observed the aqueous stream breaks into a continuous stream of droplets (FIG. 1a). Upon switching off the acoustic field, the streams return to their native coflow configuration, depicting a reversible stream-drop ($S - D$) transition. On the other hand, for $\mathrm{Ca} > 1$, stream 1 does not break and instead relocates to the channel center as a liquid thread (FIG.1b). The streams regain their native configuration when the

[1] L. Rayleigh, Proc. R. Soc. London 29, 71 (1879).
[2] A. S. Utada, A. Fernandez-Nieves,1, J. M. Gordillo, and D. A. Weitz, Phys. Rev. Lett. 100, 014502 (2008).
[3] T. Cubaud, and T. G. Mason, Phys. Fluids 20, 053302 (2008).
[4] E. Hemachandran, S. Karthick, T. Laurell, A. K. Sen, Europhys. Lett. 125, 54002 (2019).

acoustic field is turned off, depicting reversible stream-thread (S − T) transition. We characterize stream-drop transition and stream relocation in terms of the Ca of the phases. We study the growth and suppression of instability upon switching ON and OFF the acoustic field, respectively in terms of the variation of the width of the stream at the necking region and jet length with time (FIG. 2). We explain the regimes in terms of the relevant timescales and a transition between convective and absolute instability.

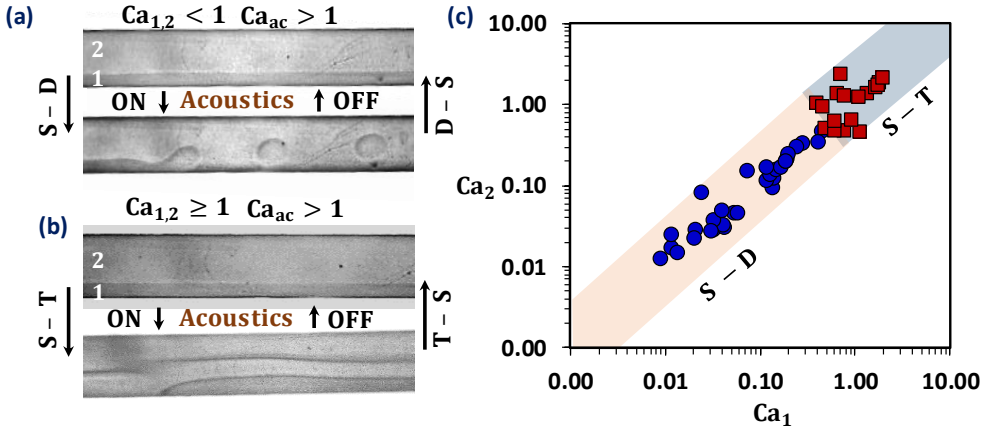

FIG. 1. Experimental images showing reversible (a) stream-drop (S-D) transition, for $Ca_{1,2} < 1$ and $Ca_{ac} > 1$, Movie 1, (b) stream-thread (S-T) trasition, for $Ca_{1,2} < 1$ and $Ca_{ac} > 1$, Movie 2. Stream 1: Aqueous glycerol (80%), Stream 2: mineral oil. (c) S-D and S-T regimes for the different combinations of fluids as streams 1 and 2.

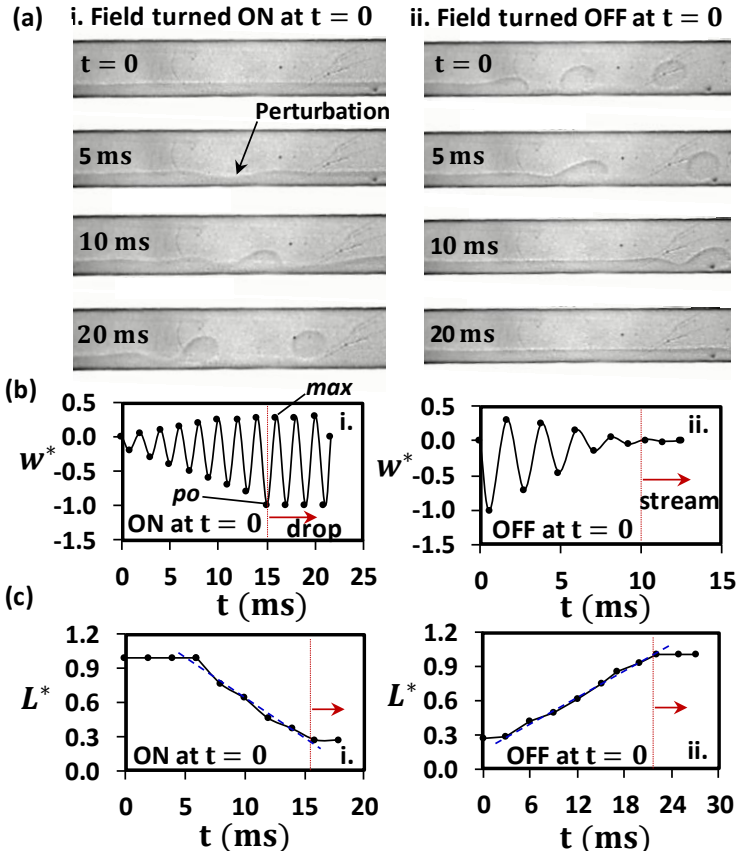

FIG. 2. (a) Experimental images showing the growth and suppression of instability upon switching (i) ON and (ii) OFF the acoustic field, respectively. (b) Variation of the dimensionless width of the stream, $w^* = (w_n - w_1)/w_1$, at the necking region with time, when the acoustic field is turned (i) ON and (ii) OFF. (c) Variation of dimensionless jet length, $L^* = (L_j/W)$, with time, when the acoustic field is switched (i) ON and (ii) OFF. Stream 1: Aqueous glycerol (80%) at flow rate 5 μL/min, Stream 2: mineral oil at flow rate 35 μL/min, applied voltage 16.1 V_{pp}, and frequency 2.1 MHz.

Reversible Transition From Ferrofluid Drop To Spikes Due To An Approaching Magnet

Sachin Kumar Jain[1], Utsab Banerjee[2], Chiranjit Mandal[3] and Ashis Kumar Sen[4]

[1] *Department of Mechanical Engineering, IIT Madras, 600036, Chennai, India* nischay91@gmail.com
[2] *Department of Mechanical Engineering, IIT Madras, 600036, Chennai, India* utsabju@gmail.com
[3] *Department of Mechanical Engineering, IIT Madras, 600036, Chennai, India* chiranjithitk@gmail.com
[4] *Department of Mechanical Engineering, IIT Madras, 600036, Chennai, India* ashis@iitm.ac.in

ABSTRACT

Ferrofluid droplet is seen to undergo surface normal instability or Rosensweig instability when its magnetization exceeds a critical magnetization and form spike like structures. We study the normal field instability-driven reversible transition from ferrofluid droplet to spikes, when a sessile ferrofluid drop is exposed to a varying magnetic field gradient due to an approaching magnet. The reversible transition is attributed to the critical magnetization of the ferrofluid and a characteristic wavelength that control the normal-field instability. We extend the theory of magnetic instability by including the non-uniformity of the field in all directions to predict the critical condition for the transition, which is in good agreement with experiments. The spacing between the spike and height and the number of spikes measured from the experiments are in agreement with the existing theory.

KEYWORDS: Normal Surface Instability, Ferrofluid, Spikes, Droplets.

INTRODUCTION

Ferrofluid (FF) spikes formation due to normal field instability[1] has been studied quite extensively though study on the effects of non-uniformity of the magnetic fields has been seldom attempted[2]. In a non-uniform field, in addition to the contributions of surface tension and gravity leading to capillary instability, the effect of the field gradient needs to be considered to explain the phenomenon, thereby accounting for the magnetic instability. The onset of normal-field instability leading to the formation of spikes is observed at a critical gap between the magnet and ferrofluid droplet.

We report for the first time the observation of a reversible transition between a droplet to spikes by exposing a sessile FF droplet to a varying magnetic field gradient due to a slowly approaching magnet. We use FF droplets of different particle concentrations and volumes and experimentally identify the conditions for the transitions. We extend the theory of normal field instability to include the magnetic field gradient in all directions, and predict the conditions for the transitions, spacing between the spikes and height and number of spikes at the different magnetic Bond numbers, and compare it with experiments. We explain the reversible transition in terms of the critical magnetization and the characteristic wavelength, $\lambda_{cx} = 2\pi\sqrt{\sigma/\alpha_x}$. The condition for instability results in an expression for the x-component of the critical magnetization, which is given as $M_{cx} = \left[\frac{4\sigma\alpha_x}{\mu_0^2}\left(1+\frac{1}{r_x}\right)^2\right]^{1/4}$, where $\alpha_x = \rho g - \mu_0 \frac{\partial H_{ax}}{\partial x}\Big|_0 \frac{M_x(H_{ax}(0))}{1+N\tilde{\chi}}$, $\tilde{\chi} = \frac{dM}{dH}\Big|_{H_a(0)}$ is the differential susceptibility and r_x is the susceptibility ratio, which is the geometric mean of chord and tangent susceptibilities, $r_x = \sqrt{\frac{H_{ax}(0)}{H_x(H_{ax}(0))}\frac{dH_{ax}}{dH_x}\Big|_{H_x(H_{ax}(0))}}$. For a non-uniform field, the surface instability occurs when the induced magnetization, M_x is higher than the critical magnetization M_{cx} leading to the formation of spikes.

---

[1] R. E. Rosensweig, *Ferrohydrodynamics*. Dover Publications, Inc., 1997.

[2] T. Vieu and C. Walter, "Shape and fission instabilities of ferrofluids in non-uniform magnetic fields," *J. Fluid Mech.*, vol. **840**, pp. 455–497, 2018, doi: 10.1017/jfm.2018.83.

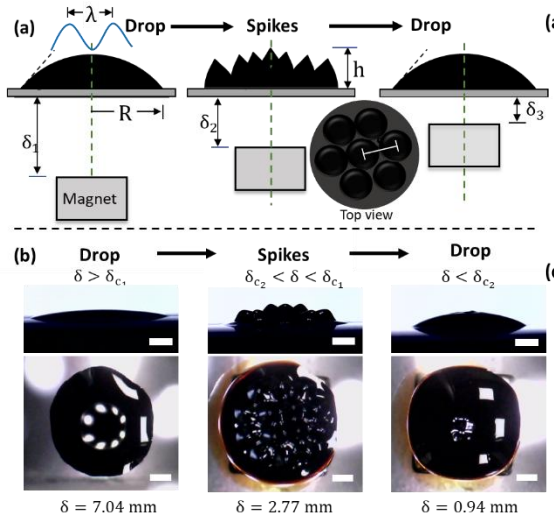

Fig. 1 (a) Schematic of reversible transition of ferrofluid (FF) drop to spikes due to a slowly approaching magnet, droplet regime is observed when $\delta > \delta_{c_1}$ and $\delta < \delta_{c_2}$, spikes are formed for $\delta_{c_2} < \delta < \delta_{c_1}$, (b) Experimental images showing reversible droplet-spikes transition for a FF drop of 10 µl volume and $M_{sat} = 3.57 \times 10^4$ A m^{-1} (8% v/v conc.), here $\delta_{c_1} = 6.5$ mm and $\delta_{c_2} = 1$ mm. Scale bar represents 1 mm.

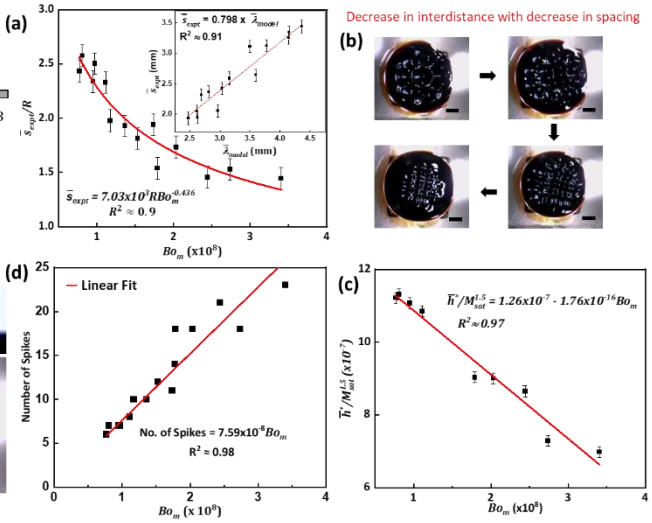

Fig. 2 (a) Variation of the area-averaged spacing $\bar{s}_{expt}$ from the experiments with the magnetic Bond number (Bo_m), The comparison of $\bar{s}_{expt}$ from experiment and characteristic wavelength $\bar{\lambda}_{model}$ predicted using model, (b) Experimental images showing a decrease in spacing between the ferrofluid spikes (s) with a decrease in drop to magnet gap, δ, (Scale bar represents 1 mm.) (c) Variation of the area-averaged height of the FF spikes with Bo_m and M_{sat}, (d) Variation of the number of FF spikes with Bo_m.

We calculated the area-averaged wavelength of the spikes as, $\bar{\lambda}_{model} = \frac{1}{l_y l_z}\int_0^{l_z}\int_0^{l_y} \lambda_{cx} dy\, dz$ and compared with the area-averaged spacing between the spikes, $\bar{s}_{expt} = \frac{1}{l_y l_z}\int_0^{l_z}\int_0^{l_y} s dy\, dz$, measured from experiments, here l_y & l_z are taken as half lengths of the cubic permanent magnet in y and z direction respectively. The model predictions and experimental values are related with a linear relation, $\bar{s}_{expt} = 0.8\,\bar{\lambda}_{model}$ with $R^2 \approx 0.91$. The combined effect of FF droplet volume, surface tension, and the magnetic field is represented in terms of the magnetic Bond number $Bo_m = RB_x M_x/\sigma$, where $R = \sqrt[3]{3V/4\pi}$, V being the drop volume. We find that the $\bar{s}_{expt}$ is related to the Bo_m following $\bar{s}_{expt} \sim Bo_m^{-0.436}$ with $R^2 \approx 0.9$. It is observed that the average height of the spikes ($\bar{h}$) gradually decreases as the magnet approaches the FF droplet, concomitant with an increase in the number of spikes and a decrease in the spacing between them. The non-dimensional average spike height $(\bar{h}^*) = \bar{h}/R_0$ is found to be related with M_{sat} and Bo_m following, $(\bar{h}^*/{M_{sat}}^{1.5}) \sim {Bo_m}^n$ with $R^2 \approx 0.97$.

ACKNOWLEDGEMENTS

A.K.S. thanks the Science and Engineering Research Board (SERB) of the Department of Science & Technology (DST), Government of India for providing financial support via Grant No. CRG/2019/000995.

Edge-based Front Tracking: a new method for tracking interfaces.

Stéphane Zaleski[1] and Léonardo Chirco[1]

[1] *Sorbonne Université and CNRS, Institut Jean Le Rond d'Alembert, France*

We propose a novel class of Edge-Based Front-Tracking Methods (EBFTM) in the field of multiphase flows for tracking the interface. The position of the interface is tracked by marker points located on the edges of the underlying grid, making the method flexible with respect to the choice of spatial discretization and suitable for parallel computation. In this paper we present a simple EBFTM based on two- dimensional Cartesian grids and on a linear interface representation. The method is described by Chirco & Zaleski (2022) and is based on an idea of Semushin (1988). The corresponding Basilisk code is also given in the References below.

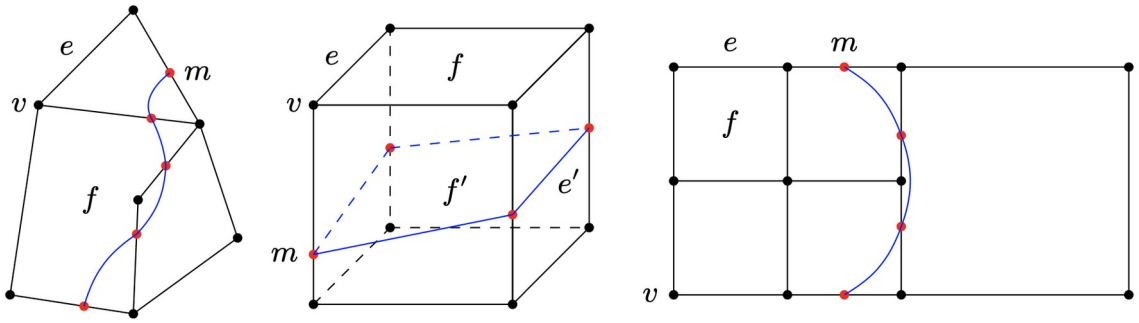

Figure 1: Schematics of Edge-Based Front-Tracking. (Left) On an unstructured planar grid formed of edges e (black lines), vertices v (black dots) and faces f (polygons delimited by black lines), the interface passes through the markers m (red dots). (Center) On a regular cuboid volume grid, with again edges e (black lines), vertices v (black dots) and faces f (squares delimited by black lines), the interface passes through the markers m (red dots). The markers m form the vertices of the surface grid tracking the interface, with edges e' and faces f' on the latter grid. The faces are in general non-planar. (Right) The leaf cells on a quadtree grid form a particular type of unstructured grid. The edges can again be the location of marker points.

References

Chirco, Leonardo, and Stephane Zaleski. "An Edge-Based Interface-Tracking Method for Multiphase Flows." *arXiv preprint arXiv:2202.06704* (2022).

S. Semushin. Rectangular grid computation of the flow with contact boundary fitting. Preprint Inst. Appl. Math. N134, 1988.

Chirco, Leonardo, code in http://basilisk.fr/sandbox/lchirco/semushin.h

Exact solutions for viscous Marangoni spreading of insoluble surfactants

Thomas Bickel[1] and François Detcheverry[2]

[1] *Laboratoire Ondes et Matières d'Aquitaine, Univ. Bordeaux, France,* thomas.bickel@u-bordeaux.fr
[2] *Institut Lumière Matière, CNRS & Univ. Lyon, France,* francois.detcheverry@univ-lyon1.fr

When a surface-active species is inhomogeneously distributed at the water-air interface, it induces a Marangoni stress that drives a liquid flow in the bulk. The time evolution of the surfactant distribution then results from a complex balance between viscous forces and surface tension gradients. Marangoni spreading is involved in many fundamental and industrial applications, including the stability of foams, the rising motion of gas bubbles, or the control of film thickness in coating processes. Surfactant spreading is also relevant in the field of active matter. Indeed, when a particle filled with surface-active molecules (*e.g.*, camphor or alcohol) is placed at the water-air interface, the resulting surface-tension gradients drive the spontaneous motion of the particle even though it is perfectly symmetric. To elucidate the actuation mechanism of these Marangoni surfers, a fine understanding of surfactant transport is therefore required [1].

Although most previous studies have focused on thin films, where the lubrication approximation applies, we consider here a semi-infinite liquid domain. The hydrodynamic signature of surfactant transport in a deep layer has been investigated recently at steady-state [2]. Regarding the dynamics, asymptotic self-similar solutions have been thoroughly discussed in the wake of the seminal work of Jensen [3]. Still, little is known regarding the transient behavior of Marangoni spreading, and exact solutions are rather sparse. Indeed, since the vorticity created by the (Marangoni) shear stress penetrates deep into the fluid, the resulting transport equations are generally both nonlocal and nonlinear. In this talk, I will explain how the coupled Stokes and advection-diffusion equations can be reduced to a single Burgers equation for a complex field. I will then present several analytical solutions for the spreading dynamics. In particular, I will show that the presence of impurities at the interface can significantly alter the dynamics, as previously observed experimentally [4] and numerically [5]. I will also show that the spreading of a surfactant "pulse" is very different from the closing of a surfactant "hole", as a consequence of nonlinearity. Finally, I will discuss under which conditions Marangoni spreading can be described in terms of an effective diffusion coefficient [6].

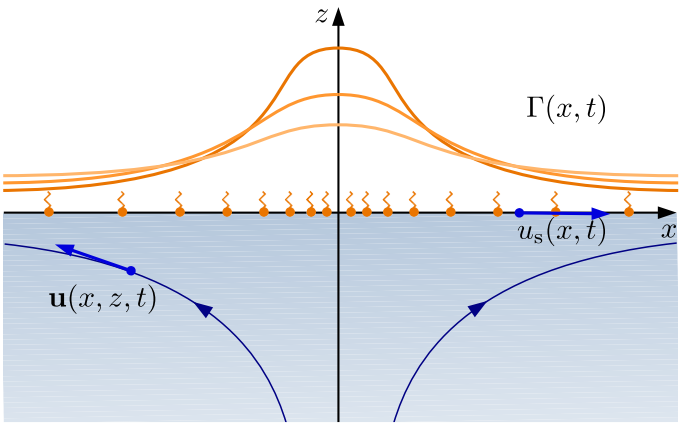

FIG. 1. Spreading of insoluble surfactants at the interface of a semi-infinite liquid layer.

[1] N. J. Suematsu *et al*., Langmuir **30**, 8101 (2014).
[2] M. Roché *et al*., Phys. Rev. Lett. **112**, 208302 (2014); M. M. Bandi *et al.*, Phys. Rev. Lett. **119**, 264501 (2017).
[3] O. E. Jensen, J. Fluid Mech. **293**, 349 – 378 (1995).
[4] M. L. Sauleda et al., Langmuir **37**, 3309 (2021) ; Y. Xu et al., Colloids Surf. A **635**, 128087 (2022).
[5] J. R. Landel *et al.*, J. Fluid Mech. **883**, A18 (2020); R. McNair, O. E. Jensen and J. R. Landel, J. Fluid Mech. **930**, A15 (2022).
[6] T. Bickel, Soft Matter **15**, 3644 (2019); T. Bickel and F. Detcheverry, *submitted* (2022).

Two examples of flows forced by acoustics or by light beam

Philippe Brunet[1], Julien Dervaux[1], Laurent Royon[2], Xiaofeng Guo[2], Aina Ramamonjy[1], Chuanyu Zhang[1,2], Geyu Zhong[1,2], Zhuo Ma[1,2]

[1] *Laboratoire Matière et Systèmes Complexes (MSC) - Université Paris Cité, UMR CNRS 7057, Paris*
philippe.brunet@univ-paris-diderot.fr

[2] *Laboratoire Interdisciplinaire des Energies de Demain (LIED) - Université Paris Cité, UMR CNRS*

We present two examples where a flow can be induced by external excitations in low-Reynolds number situations. The first one is induced by kHz-acoustic forcing within a microchannel with one or several sharp edges, which typical flow shown in Fig. 1-Left consists in a strong jet shooting out of the tip. The phenomenon of acoustic streaming is shown to be strongly enhanced near such sharp structures. We carried out extensive experiments and numerical simulations to better quantify and understand the underlying mechanisms [1]. We also quantify the mixing enhancement in an array of such sharp edges [2].

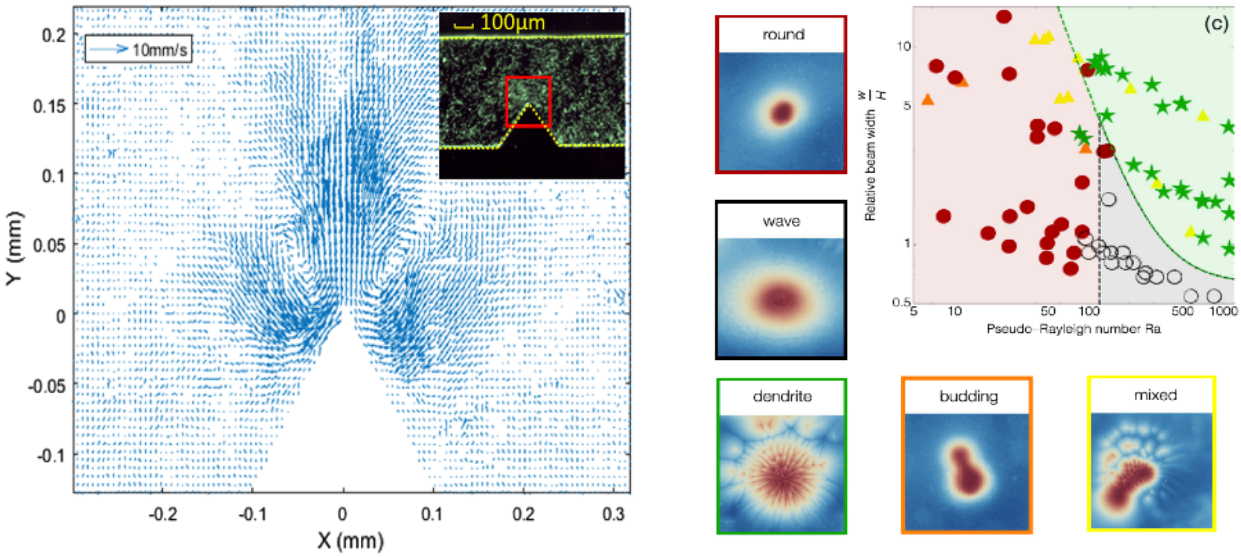

FIG. 1. Left: Velocity field of acoustic streaming near a sharp edge in a micro channel (shown as inset), (f= 2.5 kHz, Va = 37.8 mm/s, water). Right:Stability diagram (in Pseudo Rayleigh number and light beam width) of the different regimes observed in experiments of photo-bioconvection of a suspension of phototactic micro-algae subjected to local light beam. Insets around the diagram are microbes concentration profiles around the beam.

The second situation concerns a suspension of phototactic and heavy-buoyant micro algae. Having the ability to swim toward gradients of light intensity, algae accumulate in the vicinity of a thin laser beam. The resulting concentration profile can be either stationary, or show dynamical regimes involving so-called bio-convection, due to that algae are non-neutrally buoyant. Controlling both the pseudo-Rayleigh number via the suspension depth and initial concentration of microbes, and the laser beam width, we put in evidence various dynamical regimes : radial propagating waves, dendritic-like structures with a well-defined orthoradial wavelength, or budding instability as an unique finger grows and expand far away from the light beam [3,4]. Figure 1-Right show the phase diagram and corresponding regimes. Our study also allowed to quantify the phototactic response of the algae from a population dynamics, which reveals the highly non-linear response of algae with light intensity [4].

[1] C. Zhang, X. Guo, L. Royon and P. Brunet. Physical Review E 102, 043110 (2020).
[2] C. Zhang, P. Brunet, L. Royon and X. Guo. Chemical Engineering Journal 410, 128252 (2021).
[3] J. Dervaux, M. Capellazzi Resta and P. Brunet. Nature Physics DOI: 10.1038/NPHYS3926 (2017).
[4] A. Ramamonjy, J. Dervaux and P. Brunet. Phys. Rev. Lett. 128, 258101 (2022).

Droplet breakup and size distribution of satellite fragments under a swirl airstream

Someshwar Sanjay Ade[1], Pavan Kumar Kirar[2], Lakshmana Dora Chandrala[3] and Kirti Chandra Sahu[2]

[1]*Center for Interdisciplinary Program, Indian Institute of Technology Hyderabad, Sangareddy, 502 284, Telangana, India*
[2]Department of Chemical Engineering, Indian Institute of Technology Hyderabad, Sangareddy, 502 284, Telangana, India
[3]*Department of Mechanical and Aerospace Engineering, Indian Institute of Technology Hyderabad, Sangareddy, 502 284, Telangana, India*
Email: ksahu@che.iith.ac.in

Raindrops reach earth in a wide variety of shapes and sizes due to the complex interaction between droplets and the atmosphere and the accompanying microphysical processes such as fragmentation [1-2], coalescence [3], and phase change [4]. These microphysical processes are further influenced by various factors, including meteorological conditions, the airstream and cloud type from which raindrops originate, and the earth's topology. The distribution of shape and size of raindrops is one of the important factors in rainfall modelling. In this talk, we will discuss the interaction of a droplet with an airstream. In swirl flow, the droplet experiences oppose-flow, cross-flow and co-flow conditions depending on its ejection location, the velocity of the airstream and the swirl strength, which results in distinct droplet morphologies as compared with the straight airflow situation (figure 1). We observe a new breakup phenomenon, termed as 'retracting bag breakup', as the droplet encounters a differential flow field created by the wake of the swirler's vanes and the central recirculation zone in swirl airflow. A regime map demarcating the various modes, such as no breakup, vibrational breakup, retracting bag breakup and bag breakup modes, is presented for different sets of dimensionless parameters influencing the droplet morphology and its trajectory. In contrast to the straight flow, the swirl flow promotes the development of the Rayleigh–Taylor instability, enhancing the stretching factor in the droplet deformation process, resulting in a larger number of fingers on the droplet's surface. In order to gain physical insight, a theoretical analysis based on the Rayleigh–Taylor instability is proposed for the swirl flow. We will also discuss some of our recent findings obtained using an inline holography technique that provides the size distributions of satellite droplets caused by the fragmentation of a larger droplet.

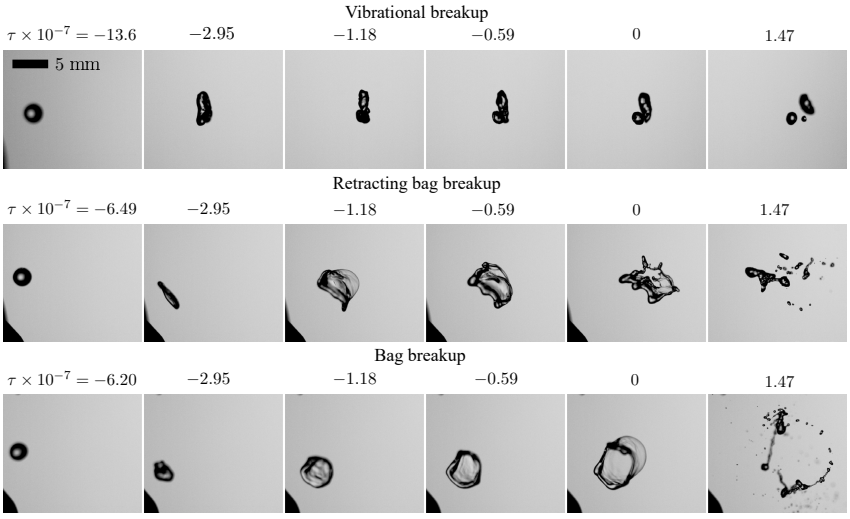

Figure 1: Effect of the Swirl number. Sw on the fragmentation process of a water droplet (obtained from shadowgraphy) for We = 12.69. Top row: Sw = 0 (vibrational breakup), middle row: Sw = 0.47 (retracting bag breakup) and bottom row: Sw = 0.82 (bag breakup).

1) Villermaux, E. & Bossa, B., Single-drop fragmentation determines size distribution of raindrops. Nat. Phys. 5(9), 697–702 (2009).
2) Kirar, P. K., Soni, S. K., Kolhe, P. S. & Sahu, K. C., An experimental investigation of droplet morphology in swirl flow. J. Fluid Mech. 938, A6 (2022).
3) Chaitanya, G. S., Sahu, K. C. & Biswas, G., A study of two unequal-sized droplets undergoing oblique collision. Phys. Fluids 33 (2), 022110 (2021).
4) Schlottke, J. & Weigand, B., Direct numerical simulation of evaporating droplets. J. Comput. Phys. 227 (10), 5215–5237 (2008).

Numerical simulations of Deforming Capsules

Kiran Satheesh[1] and Gaurav Tomar[1]

[2] *Department of Mechanical Engineering, IISc, Bangalore, India*
Email: gtom@iisc.ac.in

Capsules or cells moving through fluids are frequently encountered in nature, especially in biological systems[1]. During their motion through various flow conditions, they could deform or impact with the boundaries. Earlier studies on understanding such systems were mostly experimental or analytical and on simple configurations[2]. Recently, with the advance of computational power and development of numerical algorithms, direct numerical simulations have become a viable alternative[3]. Using an in-house developed parallel incompressible Navier Stokes solver coupled with a front tracking solver, we study two configurations of deforming capsules in flow which have wide applications.

In the first case, we look at how a capsule which directly impacts a solid surface deforms at low Reynolds numbers. We specifically investigate the effect of capsule membrane stiffness on its evolution. We have also studied the effect of membrane surface area incompressibility which is seen in most of the biological cells. Figure 1a shows an instance of a capsule which spreads after impact for a Weber number of 1 and Reynolds number of 20. Figure 1b shows the comparison of membrane model (Neo-Hookean and Skalak) on capsule evolution at high Weber numbers.

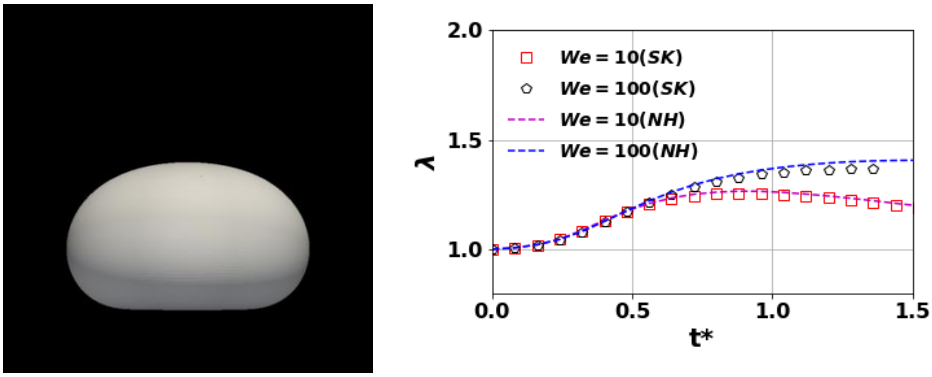

FIG. 1a) Instantaneous view of a capsule impacting a solid surface at a Weber number of 1 and Reynolds number of 20; 1b) Comparison of evolution of maximum diameter of capsule scaled with initial diameter for Neo-Hookean and Skalak models at two different Weber numbers at a Reynolds number of 10.

In the second study we propose a new approach to capsule sorting by manipulation of the flow field. We first study the effects of curvature of streamlines on evolution of capsules as they pass through constrictions. We also look at the effect of constriction width on the capsule evolution. We then show that this understanding could be made use in sorting of capsules based on their membrane stiffness. The proposed configuration is shown to have several advantages over the existing sorting methods.

REFERENCES

[1] Pozrikidis, C. (2003). *Modeling and simulation of capsules and biological cells*. Chapman and Hall/CRC.

[2] Barthes-Biesel, D., & Rallison, J. M. (1981). The time-dependent deformation of a capsule freely suspended in a linear shear flow. *Journal of Fluid Mechanics*, *113*, 251-267.

[3] Barthes-Biesel, D. (2016). Motion and deformation of elastic capsules and vesicles in flow. *Annual Review of fluid mechanics*, *48*, 25-52.

Coupled electrohydrodynamic transport in rough fractures: a generalized lubrication theory

Mainendra K. Dewangan[1], Uddipta Ghosh[1,2], Tanguy LeBorgne[2] and Yves Meheust[2]

[1] *Discipline of Mechanical Engineering, Indian Institute of Technology Gandhinagar, Palaj 382355, GJ, India*
[2] *Universite de Rennes I, CNRS, Geosciences Rennes (UMR6118), 35042 Rennes, France*

Fractures provide pathways for fluids and solutes through crystalline rocks and low permeability materials, thus playing a key role in many subsurface processes and applications. In small aperture fractures, solute transport is strongly impacted by the coupling of electrical double layers at mineral–fluid interfaces to bulk ion transport. Yet, most models of flow and transport in fractures ignore these effects. Solving such coupled electrohydrodynamics in realistic three-dimensional (3-D) fracture geometries poses computational challenges which have so far limited our understanding of those electro-osmotic effects' impact. Starting from the Poisson–Nernst–Planck–Navier–Stokes (PNPNS) equations and using a combination of rescaling, asymptotic analysis and the Leibniz rule, we derive a set of nonlinearly coupled conservation equations for the local fluxes of fluid mass, solute mass and electrical charges. Their solution yields the fluid pressure, solute concentration and electrical potential fields. The model is validated by comparing its predictions to the solutions of the PNPNS equations in 3-D rough fractures. Application of the model to realistic rough fracture geometries evidences several phenomena hitherto not reported in the literature, including: (i) a dependence of the permeability and electrical conductivity on the fracture walls' charge density, (ii) local (sometimes global) flow reversal, and (iii) spatial heterogeneities in the concentration field without any imposed concentration gradient. This new theoretical framework will allow systematically addressing large statistics of fracture geometry realizations of given stochastic parameters, to infer the impact of the geometry and various hydrodynamic and electrical parameters on the coupled transport of fluid and ions in rough fractures

Predictions of Charge and Mass Loss During the Breakup of Critically and Sub-crtically Charged Droplets

Rochish Thaokar[1], Neha Gawande[1], Mohit Singh[1] and Y.S. Mayya[1]

[1] *Department of Chemical Engineering, Indian Institute of Technology Bomaby, Mumbai, India, 400076*
rochish@che.iitb.ac.in

I. GENERAL BACKGROUND

Charged droplets generated by electro-atomization of liquids are utilized in a wide range of applications. When the charge density of these droplets is higher than a certain value, they become Coulombically unstable and undergo breakup by emitting a fraction of charge and mass in the form of a jet which further disintegrates into a cloud of micron and sub-micron sized progeny droplets. To understand this Rayleigh breakup phenomenon of a critically charged droplet and quantify the characteristics such as the exact value of charge at which the droplet shows Coulombic instability, cone angle from which jet is ejected out, the fraction of charge and mass lost in the fission process, number of progeny droplets formed and their secondary breakup, we performed systematic experiments by levitating a charged droplet in air using electrodynamic balance. All the successive events of the droplet breakup process such as surface oscillations, subsequent drop deformation, breakup, and relaxation of the drop back to spherical shape after ejection of progeny droplets have been recorded using the high-speed camera. Interestingly, experiments indicate that the levitated charged droplets break asymmetrically and predominantly in the upward direction. To understand this predominant upward breakup observed in the experiments, numerical simulations are carried out using the axisymmetric boundary element method (BEM) for both viscous and inviscid charged droplets in an AC quadrupole field. The numerical simulations in the inviscid limit accurately capture the levitation of the droplet, its surface oscillation dynamics, and the eventual breakup as a function of time in one simulation. This enables us to observe the effect of coupling between the center of mass motion of the droplet within the trap with its surface dynamics. The simulations correctly capture the evolution of the droplet from a critically perturbed shape, and the non-linear interactions of various forces show that the droplet exhibits sub-critical Rayleigh breakup and the direction of asymmetry in the breakup mainly depends on the value of charge, the critical perturbation attained by the droplet at the onset of the breakup, and the polarity of the end cap electrodes in different cycles of the applied AC field. The experimental observation of predominant upward breakup is found to be a result of 'pi' phase shift between the cycle of the applied AC field and the center of mass motion of the droplet, caused due to the presence of gravity.

II. FLOATS

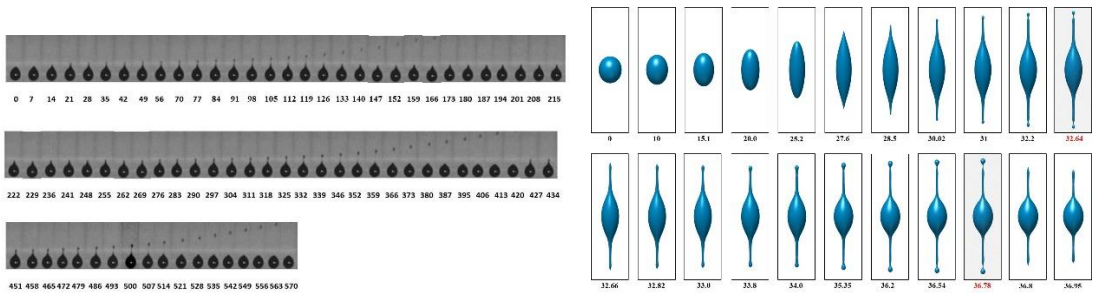

FIG. 1. Detailed pathway of droplet breakup. Left: Experimental observations; Right: Numerical simulations.

III. REFERENCES

[1] Gawande, N., Mayya, Y. S., & Thaokar, R. (2022). Effect of conductivity on the mechanism of charge ejection in Rayleigh breakup of a charged drop. *Journal of Electrostatics*, *117*, 103720.

[2] Gawande, N., Mayya, Y. S., & Thaokar, R. (2022). Translation–deformation coupling effects on the Rayleigh instability of an electrodynamically levitated charged droplet. *The European Physical Journal E*, *45*(5), 1-10.

Dynamics of Evolving Jets during Drop Impact on a Deep Liquid Pool

Santanu Kumar Das[1], Amaresh Dalal[1] and Gautam Biswas[2]

[1] Indian Institute of Technology Guwahati
[2] Indian Institute of Technology Kanpur

Abstract

A liquid droplet falling on a liquid pool may splash, coalesce or bounce back. Splashing occurs when the drop impacts the surface with a high velocity, creating a crown-like shape that breaks into several tiny droplets. Coalescence occurs owing to the falling drops having a size smaller than those are responsible splashing. The terminal velocity of such drops is also smaller. The drops of even smaller diameter and velocity lead to partial coalescence, where secondary drops are created.

The transition regimes between complete-coalescence and splashing of drops include jet formation with single or multiple secondary drops [1]. One of the main features in this regime is the formation of a central liquid jet followed by breakup of the jet in the form of drops. Earlier studies have shown that the diameter of the secondary drop lies between 0.58 and 0.94 times the diameter of the impacting drop. We perform investigations based on a coupled level-set and volume-of-fluid method to elucidate the earlier observations. The investigations reveal the creation of a variety of secondary drops depending on the impact conditions. The present study also reveals that secondary drops larger than the initial drop can be obtained at higher impact velocities [2]. We identify the importance of cavity shapes on the formation of jets and the pertaining parameters that are responsible for drop ejection.

References:

[1] B. Ray, G. Biswas and A. Sharma, Regimes during liquid drop impact on a liquid pool, ***Journal of Fluid Mechanics***, Vol. 768, pp. 492-523, (2015).

[2] S. K. Das, A. Dalal, M. Breuer, G. Biswas, Evolution of jets during drop impact on a deep liquid pool, ***Physics of Fluids***, Vol. 34, pp. 022110-1 -- 022110-10, (2022).

Hydrodynamics of Electrohydrodynamic Atomization

Archana Gupta, Bal Kishen Mishra and P. K. Panigrahi

Mechanical Engineering Department, IIT Kanpur, UP 208016

Electrohydrodynamic atomization is used for several applications i.e. micro/nano particle/capsule generation for several applications i.e. drug delivery, spray cooling and manufacturing etc. The present study experimentally investigates the hydrodynamics of the electrohydrodynamic atomization process. The role of operating parameters i.e. types of fluid, flow rate, applied electric potential in both constant (DC) and alternating (AC) mode, and the effect of actuation frequency in case of AC mode are investigated (Figure 1). The flow field is investigated using time-resolved particle image velocimetry (TR-PIV) measurements. The motion inside the Taylor cone is related to the stability of the process and the resulting size distribution of the droplets. The experiments are carried out to study the internal flow field of the Taylor cone and fluid motion surrounding the Taylor cone.

The internal flow field of the Taylor cone contains a toroidal vortex. The toroidal vortex forms in both constant and alternating actuation mode. The time-averaged velocity is higher in the case of DC actuation in comparison to the AC actuation. The flow pattern is meridional where fluid closer to the Taylor cone interface is ejected through the jet and the rest of the fluid circulates away from the apex along the axis. The surrounding fluid follows the liquid jet motion in a streamlined pattern under the action of DC voltage actuation. The nearby region at the apex of the Taylor cone is surrounded by a vortex ring in AC actuation (Figure 2). The Q-criterion is used to locate the vortical structure from PIV data. A weak vortex ring is generated at an actuation frequency of less than 100 Hz. The vortex ring spatially grows and strengthens with increasing actuation frequency for a given range of actuation frequency $100 < f_{ac} < 500$ Hz. For a frequency of greater than 500 Hz, the vortex ring starts shrinking and weakens.

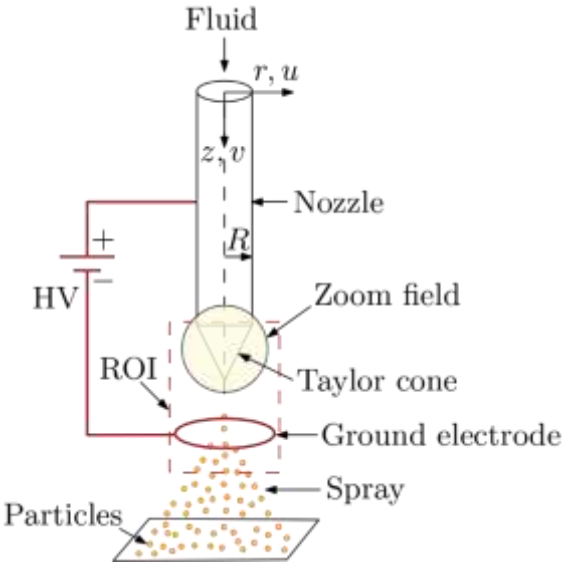

Figure 1 Schematic of the experimental setup.

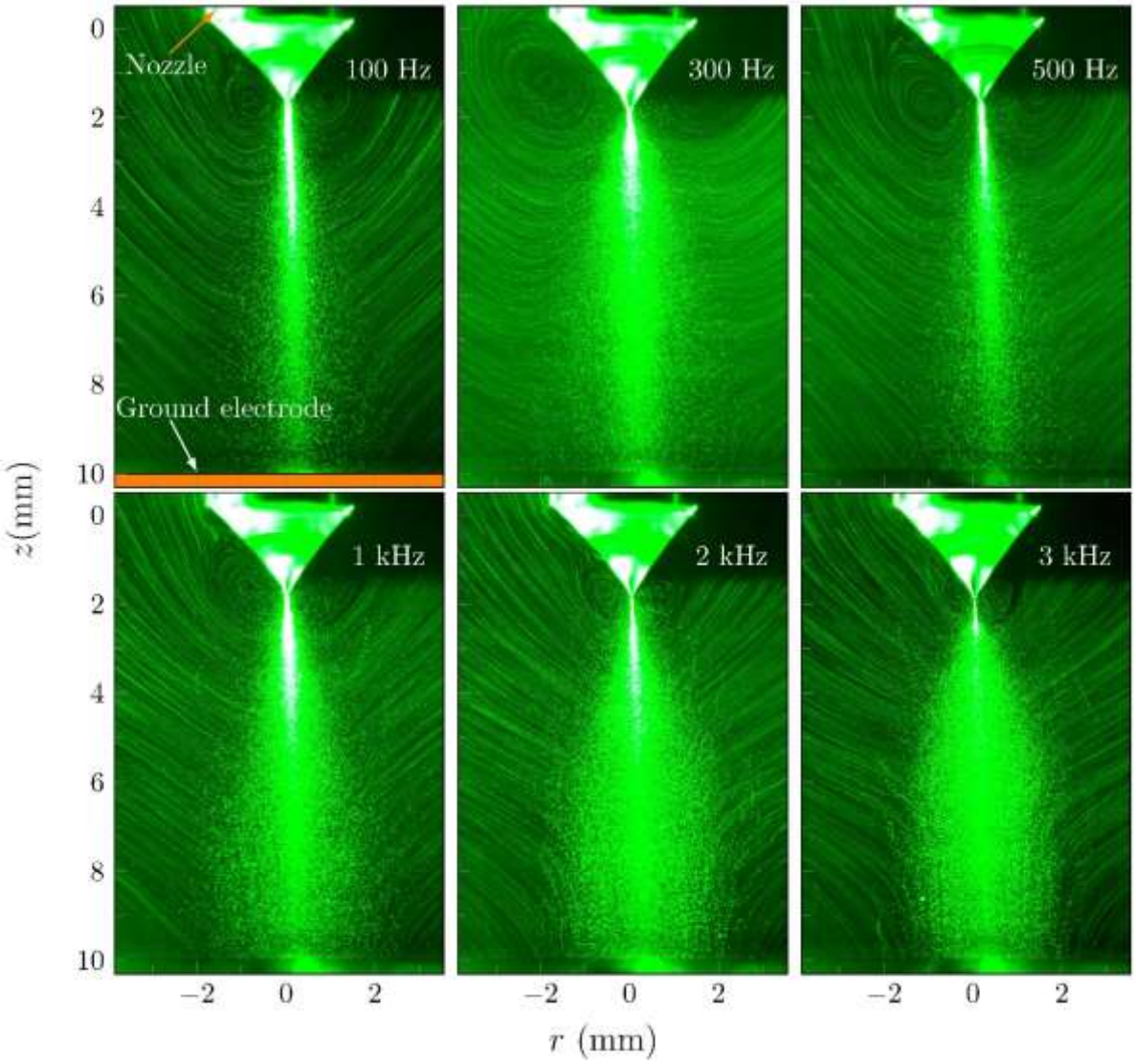

Figure 2 Instantaneous laser visualization images as a function of actuation frequency, f_{ac} in AC actuation at a constant fluid flow rate, $Q = 2\ \mathrm{ml/hr}$ and applied potential, $\phi = 5.2\ \mathrm{kV}$.

Onset characteristics of Rayleigh–Bénard–Marangoni convection in confined silicone oil - water systems

S. V. Diwakar[1]

[1]*Engineering Mechanics Unit, Jawaharlal Nehru Centre For Advanced Scientific Research, Bangalore 560064, India.* diwakar@jncasr.ac.in

The current work aims to understand the flow onset behaviour of confined two–layer systems which are under the simultaneous influence of buoyancy and thermo-capillary effects. Owing to the interfacial interactions and the possibilities of convection onset in the individual layers, these systems typically manifest diverse excitation attributes. In order to elucidate them, spectral collocation based linear and non-linear analyses has been carried out first on a sample two fluids system comprising of silicone oil and water. Resultantly, it is observed that the presence of thermo-capillarity has a differential effect on the criticality of two layer system based on its interfacial height. At higher interfacial heights, the Marangoni and buoyancy effects favour each other and result in a large reduction of critical parameters. A contrary behaviour is observed at lower heights where the two effects oppose each other to increase the corresponding critical excitation potential. In addition to these effects, the presence of thermo-capillarity is found to broaden the range of interfacial heights over which the onset of oscillatory convection can be expected in the two layers. Interestingly at these heights, modulated travelling waves have been observed amidst standing wave modes at discrete aspect ratios. This behaviour corresponds to the typical $m : n$ resonance where the critical wave numbers of convection onset in the layers are dissimilar. Following the numerical studies, a systematic experimental study has been carried out to verify the above behaviour. The experimental setup consists of a narrow cell that is sandwiched between hot and cold plates whose temperature was maintained through water circulation. The cell has provisions for changing both the fluid height ratio and the cell aspect ratio. The critical temperature for the onset of convection has been identified using a conventional z-type schlieren.

Use of patch-clamp for the investigation of the interaction force between particles and substrate

Anna IPATOVA[1], Farzam ZOUESHTIAGH[1]*, Alexis DUCHESNE[1], Maureen DELEPLACE[2], Christine FAILLE[2], Corenthin LEROY[3], Harunori YOSHIKAWA[4], Pascal MARIOT[3]

[1]Univ. Lille, CNRS, UMR 8520 - IEMN, F-59000 Lille, France
[2]Univ. Lille, CNRS, INRAE, ENSCL, UMET, F-59650, Villeneuve d'Ascq, France
[3]Univ. Lille, INSERM U1003, Bâtiment SN3, F-59655 Villeneuve d'Ascq, France
[4]Institut de Physique de Nice - UMR 7010, 1361 Route des Lucioles - 06560 Valbonne, France
**e-mail: farzam.zoueshtiagh@univ-lille.fr*

Introduction. The force of interaction between bacteria and materials is an essential factor in the understanding of phenomena at interfaces and has been studied experimentally for years. In the current work, we present an original method deriving from the patch-clamp technique to measure this interaction force.

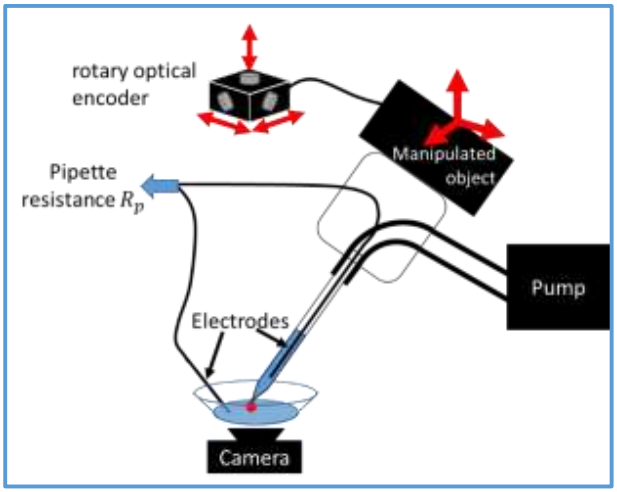

Materials and methods. Briefly, a micropipette is brought into contact with an adherent particle under the optical microscope. A given aspiration pressure is then applied and the pipette is pulled away from the particle at a given rate. If the particle does not detach, a higher aspiration pressure is applied and the experiment is repeated until the particle detach. The minimum pressure, allowing the detachment is used to calculate the interaction force between the particle and the substrate. This technique was applied to hydrophilic and hydrophobic microspheres with diameter of about 2 µm placed on an hydrophilic substrates Same technique was also used to measure the interaction force of *Bacillus* spores placed on the hydrophilic substrate: B. cereus 98/4 spores (hydrophobic, surrounded by a soft membrane called "exosporium"), *B. subtilis* PY79 (hydrophilic, surrounded by a mucous layer called "crust") and *B. subtilis* PY79 *ΔspsA* (a recombinant strain deleted in *spsA*, modified at the "crust" level, which makes the spores hydrophobic).

Results. A huge variability was first observed on the force required to detach the two microspheres from the substrate. Therefore, our results demonstrated that the hydrophilic microspheres were less adherent (average interaction force = 0.07 nN) on the hydrophilic substrate than the hydrophobic microspheres (4.62 nN), which suggests a major role of the hydrophilic/hydrophobic character of the particle on the interaction strength. A series of measurements was then performed with *Bacillus* spores. The hydrophilic *B. subtilis* PY79 spores placed on hydrophilic substrate were much less adherent (0.21 nN) than the hydrophobic *B. cereus* 98/4 (48.79 nN) or *B. subtilis* PY79 *ΔspsA* (43.86 nN). Again, it seems that the preponderant parameter is the hydrophilic/hydrophobic character of the particle while the nature and structure of the spore surface did not seem to play a significant role on the interaction strength between spores and material.

Significance. The presented technique is a part of single-cell manipulation methods. It will allow to investigate the role of different parameters that can affect the interaction forces (material and particle properties, drying time...), but also to determine the dispersion of these forces within a population.

Interfacial tension playing role in cleaning oil spills from ocean

Bahni Ray[1] and Ghulam Rabbani[2]

[1] *Department of Mechanical Engineering, IITD, Hauz Khas, 110016, India* bray@iitd.ac.in

[2] *Department of Mechanical Engineering, IITD, Hauz Khas, 110016, India* Ghulam.Rabbani@iitd.ac.in

The removal of very thin layer of oil over the ocean surface is a challenging task. Surfactants cause disintegration of this oil accumulations, creating smaller droplets with high surface-to-volume ratios, which are more accessible and easier to degrade by microorganisms. When water droplet impacts the multicomponent layer of oil above water system, the dominating capillary force helps in breaking the oil layer to micron sized oil drops. In presence of surfactant over the oil layer, the interfacial tension reduces which produces submicron and nanosized oil drops. Similar disintegration is observed when bubble moving from below bursts the multilayer. One such example is shown in FIG.1, where the bubble takes with it a layer of heavier fluid which eventually burst out. Feng et. al. [1] show bubble bursting at air/oil/water with surfactant interface can disperse submicrometer droplets of oil in water. Feng et al. [2] show the formation of oil in water nanoemulsion. The lipophilic /amphiphilic material is put in the oil phase and when the bubble approaches the water/oil with surfactant interface the bursting of the bubble leads to the formation of oil in water nanoemulsion with lipophilic material inside the oil droplets and amphiphilic molecules at the oil/water interface.

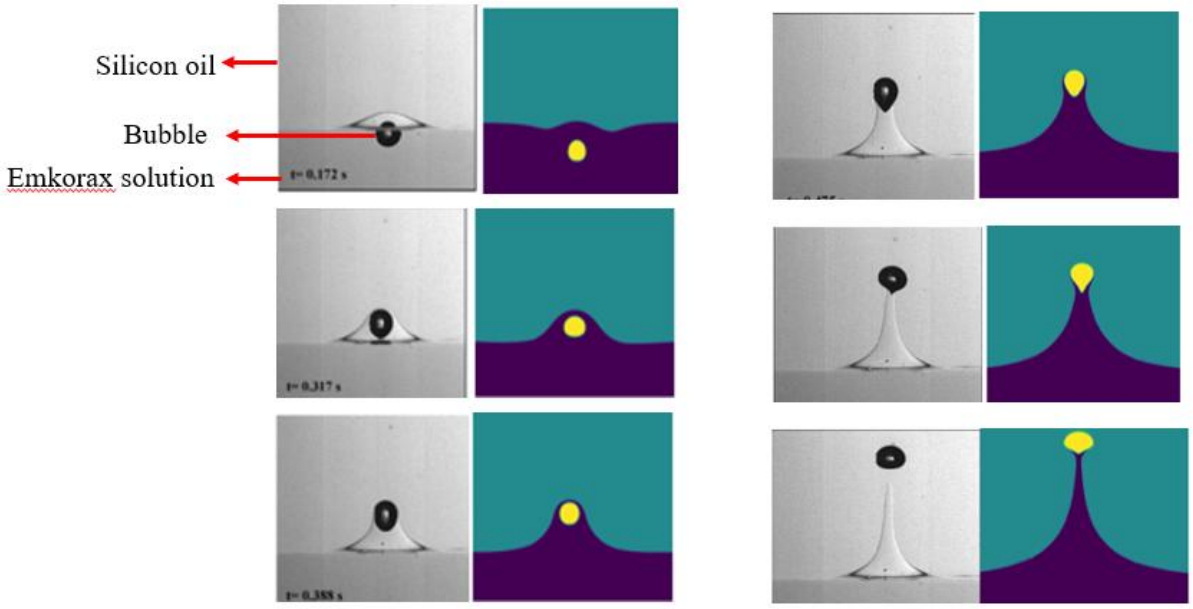

FIG. 1. Bubble bursting in presence of multicomponent fluid system. Left: time frame top to bottom; Right: time frame top to bottom.

[1] Feng, J., Roché, M., Vigolo, D., Arnaudov, L. N., Stoyanov, S. D., Gurkov, T. D., Tsutsumanova, G. G., and Stone, H. A, Nanoemulsions Obtained via Bubble-Bursting at a Compound Interface, Nature Physics **10(8)**, 606 – 612 (2014).

[2] Feng, J., Nunes, J. K., Shin, S., Yan, J., Kong, Y. L., Prud'homme, R. K., Arnaudov, L. N., Stoyanov, S. D., and Stone, H. A., A Scalable Platform for Functional Nanomaterials via Bubble-Bursting, Advanced Materials, **28(21),** 4047-4052 (2016).

Phase transition of miscible/immiscible binary fluids with the phase field approach

M. Bestehorn[1], D. Sharma[2], R. Borcia[1], S.Amiroudine[2]

1 Institute of Physics, Brandenburg University of Technology, 03044 Cottbus, Germany
2 Université Bordeaux, I2M UMR Centre National de la Recherche Scientifique 5295, Talence, F-33400

This work concerns the study of binary fluids with a phase field approach. The modified Cahn-Hilliard equation is proposed to take into account the continuous path from the immiscible state to the miscible state as defined by the species diffusion equation. For this, we consider immiscible binary fluids for temperatures below the critical temperature and miscible above. Surface tension and interface thickness vary with distance from the critical point through a temperature-dependent variable. The whole system is mechanically excited showing the Faraday instability of a planar interface. A linear Floquet analysis shows the well-known Arnold's tongues as a function of the critical temperature and the thickness of the fluid layer. Numerical simulations with finite differences method were carried out, making it possible to model nonlinear flows in the miscible and immiscible phases. Linear theory and non-linear simulations show interesting results such as the decrease in the wavelength of Faraday waves or a shift in the critical vibration amplitude when the critical temperature is approached.

To illustrate the model described above, the stability curve of the Faraday instabilities has been represented when the system is subjected to a vertical vibration of amplitude "a" and frequency ω=100 rad/s for a pair of binary fluids FC72/silicone oil. We retrieve Arnold tongues for different thicknesses of layers of fluid "d" and for and one case for $r = 0.1$ $r = 1$ (r is a control parameter vanishing at the consolute temperarure). We note that for this last case, the wavelength decreases which was confirmed during this simulation (graph on the right). In this graph, we impose $r = 1$ until t=5.72s, we then obtain standing waves which oscillate in a harmonic way then we switch to $r = -0.1$ (case of miscible fluids) and we see the change in the wavelength as a function of time until diffusion takes over and the two layers become almost perfectly mixed.

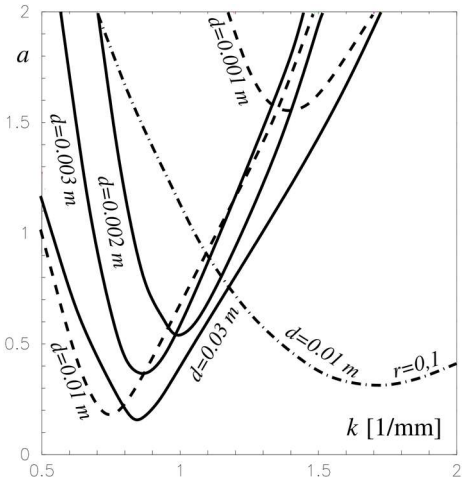

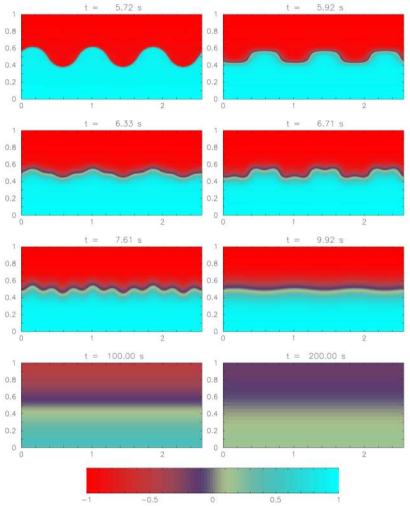

REFERENCES

- J. W. Cahn and J. E. Hilliard, "Free Energy of a Nonuniform System. I. Interfacial Free Energy", The Journal of Chemical Physics 28, 258 (1958).
- D. Jacqmin, "Calculation of Two-Phase Navier-Stokes Flows Using Phase-Field Modeling", Journal of Computational Physics, Volume 155, Issue 1, p. 96-127, (1999).
- D. Jasnow, J. Vinals, "Coarse-grained description of thermo-capillary flow", Phys. Fluids 8, 660 (1996).
- V. Jajoo, "Faraday instability in binary fluids" [PhD thesis, University of Bordeaux]. Open archives, https://tel.archives-ouvertes.fr/tel-01695491, (2017).
- Diwakar, S. V., Zoueshtiagh, F., Amiroudine, S., & Narayanan, R., "The Faraday instability in miscible fluid systems", Physics of Fluids 27(8), (2015).
- Bestehorn, M. Sharma, D., Borcia, R., and Amiroudine, S., Faraday instability of binary miscible/immiscible fluids with phase field approach, Phys. Rev. Fluids 6, 064002, (2021).

The Yoga of Droplets

Aloke Kumar[1]*

[1] Department of Mechanical Engineering, Indian Institute of Science, Bangalore

*Email: alokekumar@iisc.ac.in

Coalescence is an energy minimization phenomenon in which two drops undergoe a thermodynamic process to attain a final equilibrium state i.e. the coalesced state. Under experimental conditions, this pheonomenon can be attained in three configurations namely, sessile-pendant, sessile-sessile and pendant-pendant. For macromolecular fluids like polymer solutions, this phenomenon is complex due to the presence of molecular relaxations. In sessile-pendant configuration, we unveil the existence of three regimes on the basis of concentration ratio (c/c*) namely, inertio-elastic $c/c^*<c_e/c^*$, viscoelastic $c_e/c^*<c/c^*<20$ and elasticity dominated regime $c/c^*>20$. Our results suggest that the neck growth with time (t) follows a power law behaviour t^b, such that *b* has an universal value of 0.37 in inertio-elastic and viscoelastic regimes, followed by a monotonic decrease in the elasticity dominated regime. In this latter regime of monotonic decrase in *b*, we propose a new measurement technique called Rheocoalescence to obtain the relaxation time of the fluid.

In comparison, coalescence in sessile-sessile configuration is relatively more complex due to the presence of interface. We observe that in such configuration, coalescence can be tiggered by volume filling method (VFM) or droplet spreading method (DSM). Similar to sessile-pendant configuration, we identify four different regimes namely, inertial dominated (ID), inertio-elastic (IE), viscoelastic (VE) and elasticity dominated (ED) regimes on the basis of c/c*. Our results reveal that the temporal evolution of bridge height for VFM follows a power law behaviour, such that *b* remains constant at 2/3 in ID, IE, VE, followed by a monotonic decrease in ED. Whereas, in DSM, *b* registers a continuous decrease from *2/3* in IE, followed by a steady value of 1/2 in VE and ED. Finally, the experimental resutls are validated theoretically and numerically using the modified thin film equation obtained from linear Phan-Thein-Tanner (PTT) constitutive equation under lubrication approximation.

Evaporation-based Detection of Adulterants in Milk

Susmita Dash, Assistant Professor, Department of Mechanical Engineering
Indian Institute of Science, Bangalore 560012

Adulteration of milk poses a severe health hazard. Existing methods for detection of adulterants such as water, urea, ammonium sulfate, oils, and surfactants in milk are selective and expensive, and are often difficult to implement in rural areas. It is, therefore, crucial to develop adulterant-detection techniques that are scalable and easy to use. We have recently developed an evaporation-based low-cost technique for the detection of adulterant, specifically, added water, urea, salts, and oil in milk. We observe a specific pattern formation of nonvolatile milk solids deposited at the end of the evaporation of a droplet of unadulterated milk. These patterns alter with the addition of different adulterants. The evaporative deposits are dependent on the nature and concentrations of the adulterants added. This method can be used to detect added water in excess of 20% and a urea concentration as low as 0.4% in milk. The dataset comprising of images of evaporative deposits is used to develop a deep learning algorithm that deploys a convolutional neural network to classify the distinct evaporation patterns obtained for different types and concentrations of the adulterants. While milk is a complex fluid and adulteration may not be restricted to only water, salts, oil or urea, this evaporation-based method opens up an avenue to explore the dependence of deposition pattern on the composition of milk and use it as a low-cost physical detection tool that in conjunction with machine learning can be used for the detection of adulterants at home or at any remote location.

Shock-droplet interactions

Saptarshi Basu
Indian Institute of Science, Bangalore

Droplet atomization through aerobreakup is omnipresent in various natural and industrial processes. Atomization of Newtonian droplets is a well-studied area; however, non-Newtonian droplets have received less attention despite their frequent encounters. By subjecting polymeric droplets of different concentration to the induced airflow behind a moving shock wave, we explore the role of elasticity in modulating the aerobreakup of viscoelastic droplets. Three distinct modes of aerobreakup are identified for a wide range of Weber number (10^2-10^4) and Elasticity number (10^(-4)-10^2) variation; these modes are- vibrational, shear-induced entrainment and catastrophic breakup mode. Each mode is described as a three stage process. Stage-I is the droplet deformation, stage-II is the appearance and growth of hydrodynamic instabilities, and stage-III is the evolution of liquid mass morphology. It is observed that elasticity plays an insignificant role in the first two stages, but a dominant role in the final stage. The results are described with the support of adequate mathematical analysis.

Modeling of Gas flow at finite Knudsen number

Santosh Ansumali

Jawaharlal Nehru Centre for Advanced Scientific Research (JNCASR)

Gas flow at microflow, where Knudsen number is finite, often requires the use of either a full atomistic tool such as Direct simulation Monte Carlo (DSMC) or working with model equations such as Boltzmann BGK or Fokker Planck equation. These are expensive methodologies for simulations for long microchannels. It would be ideal to have analytical solutions for a few simplified boundary value problems and possibly a multiscale procedure to simulate realistic setups. We present a set of closed-form solutions for boundary value rarefied gas flow. Furthermore, we introduce a two-way coupling between microscopic methods such as DSMC and mesoscale method Lattice Boltzmann. We show the resulting computational gains through simulations in the laminar no-slip, transitional and turbulent regimes.

Effect of reduced shear stress on endothelial cell

Mehdi Inglebert[1], Kumari Priti Sinha[2], Lionel Bureau[1] and Chaouqi Misbah[1]

[1]*Laboratory of Interdisciplinary Physics, University of Grenoble, France*
[2]*Department of Biochemical Engineering and Biotechnology, Indian Institute of Technology Delhi, India*

ABSTRACT

The vascular endothelium is a monolayer of specialized cells that lines the inner surface of blood vessels. It is essential to maintain blood and vascular homeostasis through its functions in biochemical signaling, in vasomotion, and as a selective barrier controlling transport across and interactions with the vessel walls [1, 2]. Being in direct contact with the blood flow, Endothelial Cells (ECs) have been shown to adapt to the hemodynamic forces to which they are exposed [1–3]

Over the past 40 years, a breadth of studies have investigated the influence of fluid shear stress on the behavior and function of endothelial cells and demonstrated the importance of the level and pattern of shear stress on, e.g., EC morphology, proliferation, gene expression or the development of vascular pathologies.

Reduced blood flow, as occurring in ischemia or resulting from exposure to microgravity such as encountered in space flights, induces a decrease in the level of shear stress sensed by endothelial cells forming the inner part of blood vessels. In the present study, we use a microvasculature-on-a-chip device in order to investigate in vitro the effect of such a reduction in shear stress on shear-adapted endothelial cells (Fig. 1). We find that, within 1 h of exposition to reduced wall shear stress, human umbilical vein endothelial cells undergo reorganization of their actin skeleton with a decrease in the number of stress fibers and actin being recruited into the cells' peripheral band, indicating a fairly fast change in the cells' phenotype due to altered flow [4].

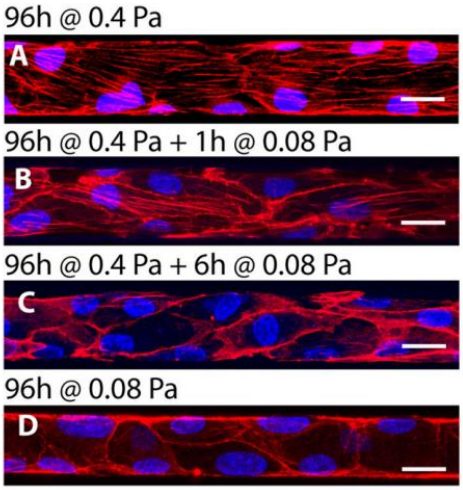

FIG. 1. From A to D, the effect of reduction in shear stress from physiological value to five-fold reduced value on actin-cytoskeleton reorganization

REFERENCES

[1] J. J. Chiu and S. Chien, Physiol. Rev. 91, 327 (2011).
[2] P. F. Davies, Nat. Rev. Cardiol. 6, 16 (2008).
[3] S. Chien, Am. J. Physiol. Heart Circ. Physiol. 292, H1209 (2007).
[4] M Inglebert, L Locatelli, D Tsvirkun, Priti Sinha, J A Maier, C Misbah, and L Bureau, Biomicrofluidics 14, 024115 (2020).

Blood Flow and Biochemical Signaling

Chaouqi Misbah, Mehdi Abbasi, Zhe Gou, Ananta Nayak, Priti Kumari Sinha[2], Sovan Lal Das[3]

[1] Université Grenoble Alpes, CNRS, LIPhy, Grenoble, France
[2] Department of Biochemical Engineering and Biotechnology, Indian Institute of Technology Delhi New Delhi India
[3]Indian Institute of Technology Palakkad, Palakkad, Kerala, India.

In this talk we will present recent theoretical and experimental studies on red blood cells (RBC) under flow. More precisely, we will consider RBC aggregation under flow and show unexpected phase diagram of aggregates formation where even for a weak adhesion energy the aggregate can be very stable, due to a subtle shape adaptation of RBCs (Fig.1). Studies will focus on low and high hematocrit, both in simple and complex geometries. We will also discuss ATP release by RBCs as well as calcium generation by endothelial cells. Finally, the focus will be directed towards experiments where it is shown that a cleavage of RBCs glycocalyx can dramatically affect aggregation processes. Several blood diseases (e.g. diabetes) are known to be associated with glycocalyx cleavage. We propose that this may strongly contribute to blood occlusion. Finally, we will present a device about blood clogging, besides making a link with crowd movement, may constitute a precious and very cheap tool for measuring adhesion energy between cells.

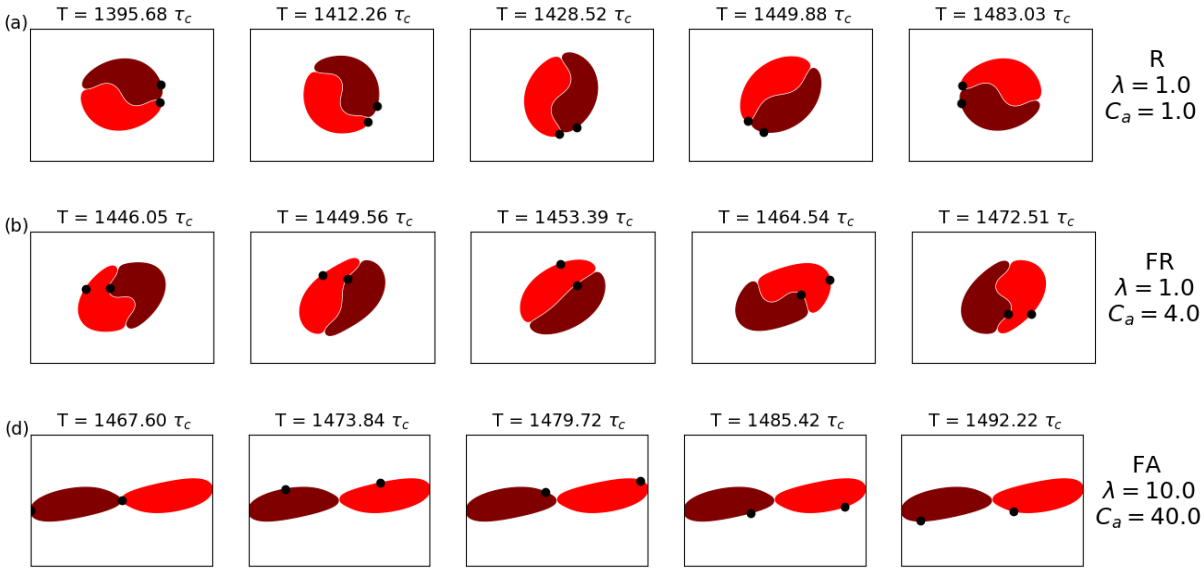

FIG. 1. Snapshots showing the dynamics of cell doublet for different capillary number C_a and viscosity contrast λ. R=rolling, FR=flexible rolling, FA=flow alignment.

.

Spontaneous shell formation during gelation by membrane-free osmosis

E. Guilbert, C. De Loubens, A. Vilotte and H. Bodiguel

Univ. Grenoble-Alpes, CNRS, Grenoble INP, Lab. Rheology and processes UMR, Grenoble, France

hugues.bodiguel@univ-grenoble-alpes.fr

Many biosourced hydrogels could be obtain thanks to the addition of calcium ions to a suspensions of oligosaccharides, glycopolymers or protein aggregates. Despite being highly permeable to water and to ions, we show in this work that those hydrogels exhibit partially selective properties to calcium ions. This selectivity – though small – lead during gelation to osmotic flows which can be used to modify the volume fraction field and to spontaneously form dense shells.

We developed a simple experimental approach to study this phenomenon. A glass capillary tube was initially filled with a colloidal suspension, and then put into contact with a concentrated calcium solution. Calcium ions progressively diffused into the glass and triggered the gelation. The gel front could be deduced thanks to standard or fluorescence microscopy. The kinetics was well accounted by a diffusion-reaction model, with a 1st order reaction scheme (see Fig1C).

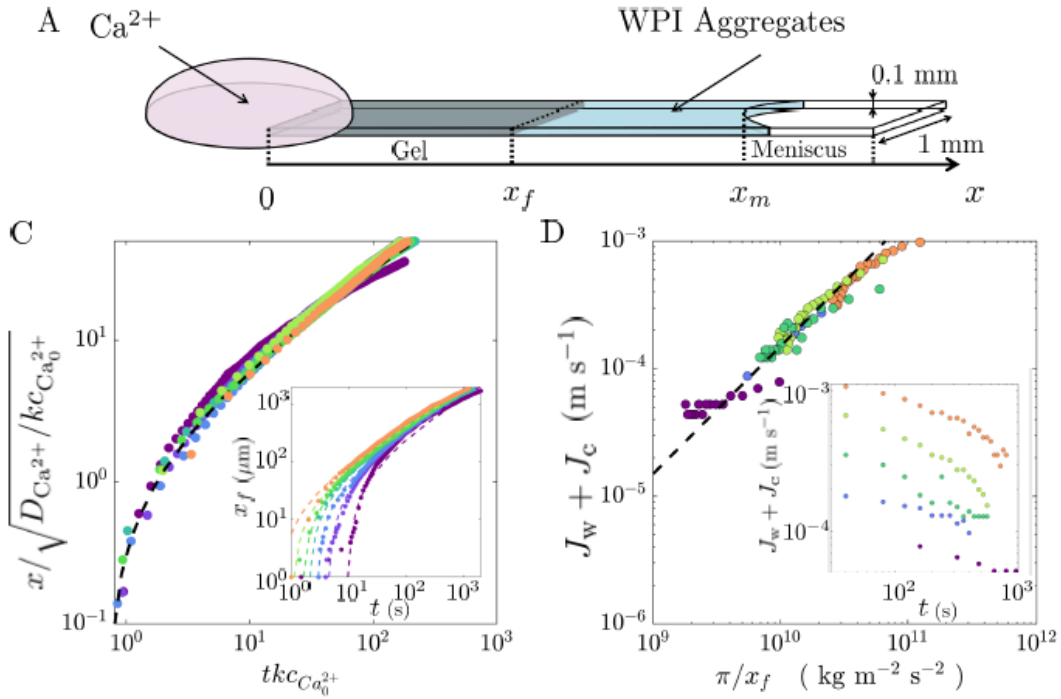

FIG. 1. A: Scheme of the experimental setup. C: Adimensional gel width versus reduced time for various calcium concentration, fitted by the prediction of a reaction-diffusion model (system: whey protein aggregates). D: Solution backward velocity as a function of the ratio of the osmotic pressure over the gel width.

Simultaneously and more unexpectedly, a net backward flow of water was observed by following tracer particles or by following the meniscus position. This flow rate was proportional to the calcium osmotic pressure and inversely proportional to the gel width, which strongly support that this flow was osmotic and that the gel formed was partially selective to calcium ions. This also implied that both the permeability and the selectivity of the gel were roughly constant and independent on the calcium concentration.

These conclusions were confirmed by applying a pressure at the free outlet of the capillary. The flow rate was found to be proportional to this applied pressure, but with an offset corresponding to a fraction of the osmotic pressure. These last experiments were thus well accounted by Kedem-Katchalsky

equations and allowed the determination of both the reflexion coefficient and the permeability of the gel. Depending of the type of material used (Alginate, Prectins and whey protein aggregates were tested), the permeability ranged from 10^{-14} to 10^{-12} m^2, and the reflexion coefficient from 10^{-4} to 10^{-2}.

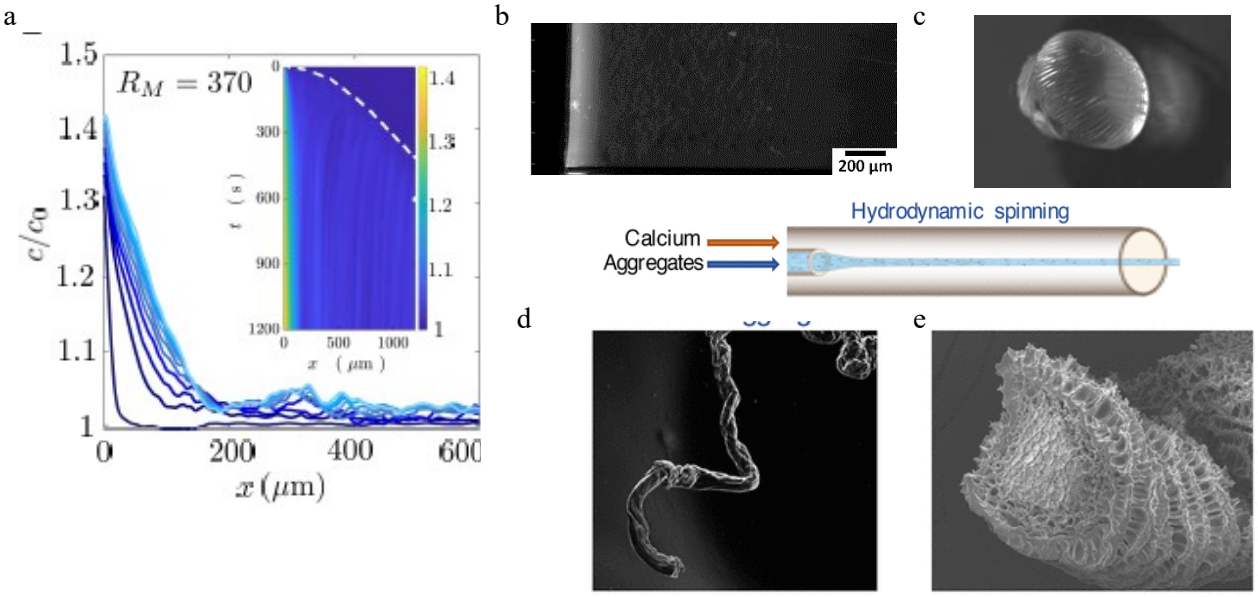

FIG. 2. a) concentration profiles of protein at different times (in insert, spatio-temporal diagram of the protein concentration). b) fluorescence image showing the shell formed in a gel of protein a protein aggregates. c) elastic capsule formed by gelation of a pectin susupension in a calcium bath. d) fiber of protein aggregate, exhibiting a core-shell structure as shown in the MEB image in e) obtained with a cutted fiber.

The osmotic flow could be used to control the spontaneous formation of a dense layer, a shell, in contact with the calcium reservoir. The osmotic flow carries materials towards this interface and thus increases the local concentration of the colloids. This phenomenon was studied in detail in the setup shown in Fig. 1. Fig2 a) and b) displays concentration profiles obtained by fluorescence microscopy. A strong gradient was evidenced close the interface, and a small increase of the concentration was observed inside the gel. Knowing the osmotic flow properties, a simple model could be proposed to account for the formation of this shell.

This mechanism could be used in other geometries in order to form core-shell structures. For example, in Fig. 2C, a droplet of pectin is produced in calcium bath which trigger its gelation. Some wrinkles appeared at the surface, strongly suggesting the existence of a rigid shell at the periphery. Another example is displayed in Fig. 2 and concern fibers, produced by hydrodynamic spinning (see scheme in Fig 2). In this example again, a shell is formed and is evidenced by electronic microscopy.

In conclusion, we have shown that bio-hydrogels act as partially selective membrane, even during the gelation process, and that this property could be of great interest to produce structured objects such as core-shell capsules or fibers, when coupled to hydrodynamic shaping.

Stretched vesicles transport uniquely across constricted microfluidic pathways

Tanoy Kahali[1], Devi Prasad Panigrahi[1], and Suman Chakraborty[1]

[a]*Department of Mechanical Engineering, Indian Institute of Technology; Kharagpur, Kharagpur, West Bengal-721302, India, Email: suman@mech.iitkgp.ac.in*

Abstract

Constriction in the flow passage in the physiological circulatory system is central to the occurrence of several diseased conditions such as thrombosis and is also pivotal to the understanding of regulatory processes activating the control of blood pressure in human vasculature. The underlying physics appears to be delicately modulated by an intriguing stretching dynamics of the encapsulated cellular materials amidst hydrodynamic focusing, an aspect that remains poorly understood thus far. Here, we bring out the exclusive role of the geometric features of a lipid vesicle to delineate different stretching transitions in a constricted microfluidic channel. These results demonstrate the strong dependency of the observed morpho-dynamics on the viscosity contrast between the inner and the suspending fluid medium and the elastic properties of the separating membrane, and open up new possibilities towards predicting diseased conditions based on exclusive image analytics characterizing their morphological transitions in a label-free paradigm.

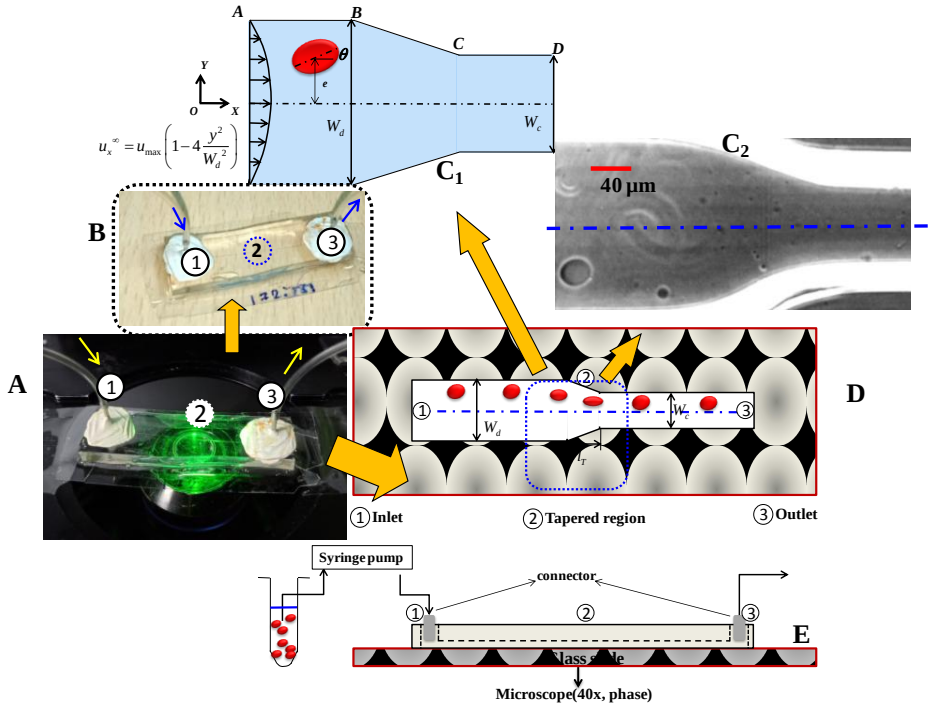

Fig. 1. Study of vesicle dynamics, modulated by a constricted microfluidic passage. (A), (B) Experimental setup for the study of constriction-driven shape dynamics in microfluidic chip labeled with inlet (1), outlet (3), and the test section (2) and observed under a transmission microscope operated in phase-contrast mode. The direction of flow has been shown using arrows. Section (C_1) shows the schematic of the problem, clearly demarcating the imposed flow profile. W_d and W_c denote the width of the diverging section (AB) and constricted section (CD), respectively. BC denotes the tapered region. The coordinate axis is located at the channel centerline. Figure (C_2) shows the experimental test section (denoted by 2 in Fig-A, B). The Channel centerline and scale bar have been marked clearly. Section (D) and (E) denote the schematic of the microfluidic channel and the experimental setup. The Blue dotted line in figure D denotes the test section.

A biophysical model explains the size distribution of circulating tumor cells in blood vessels during metastasis

Federico Bocci[1], Mohit Kumar Jolly [2] and Jose Onuchic[1]

[1] *Center for Theoretical Biological Physics, Rice University, Houston 77030, USA*
[2] *Centre for BioSystems Science and Engineering, Indian Institute of Science, Bangalore 560012, India,* mkjolly@iisc.ac.in

Migration from the primary tumor is a crucial step in the metastatic cascade. Cells with various degrees of adhesion and motility migrate and are launched into the bloodstream as single circulating tumor cells (CTC) or multicellular CTC clusters. The frequency and size distributions of these clusters have been recently measured, but the underlying mechanisms enabling these different modes of migration remain poorly understood. We present a biophysical model that couples the phenotypic plasticity enabled by the epithelial-mesenchymal transition (EMT) and cell migration to explain the modes of individual and collective cancer cell migration. This reduced physical model captures how cells undergo a transition from individual migration to collective cell migration and robustly recapitulates CTC cluster fractions and size distributions observed experimentally across several cancer types, thus suggesting the existence of common features in the mechanisms underlying cancer cell migration. Furthermore, we identify mechanisms that can maximize the fraction of CTC clusters in circulation. First, mechanisms that prevent a complete EMT and instead increase the population of hybrid epithelial/mesenchymal (E/M) cells are required to recapitulate CTC size distributions with large clusters of 5 to 10 cells. Second, multiple intermediate E/M states give rise to larger and heterogeneous clusters formed by cells with different epithelial-mesenchymal traits. Overall, this biophysical model provides a platform to continue to bridge the gap between the molecular and biophysical regulation of cancer cell migration and highlights that a complete EMT might not be required for metastasis [1].

[1] F. Bocci, M. K. Jolly, J. N. Onuchic, A biophysical model uncovers the size distribution of migrating cell clusters across cancer types, *Cancer Research* (2019); 79 (21): 5527-35.

In silico experiments modelling disendothelization in an axisymmetric idealized artery, with application to intimal hyperplasia development

J. Jansen[1], X. Escriva[1], F.S. Godeferd[1] and P. Feugier[2]

1 Fluid mechanics and acoustics laboratory, CNRS-UCBL-INSA-ECL Lyon, France
2 University Hospital Lyon South, UCBL, Villeurbanne, France

We study the role of hemodynamics and of different kinds of disendothelization on the physiopathology of intimal hyperplasia, which is a pathology appearing in high performance athletes doing long-distance sports, e.g. cycling or running. The approach is a multi-scale bio-chemo-mechanical model of an idealized axisymmetric artery that suffers either localized disendothelization or more diffuse one. The model predicts the spatio-temporal evolution of the lesions development, and grasps the short-time behavior of the damaged zones, after a few days, as well as longer-time asymptotic evolution after weeks or months. It permits to follow the evolution of macroscopic quantities, with results consistent with experimental data, in terms of sensitivity of the lesion to pathology-protective or pathology-promoting zones. It also highlights the primal importance of the initial damage on the morphology of the incipient stenosis, and of the local wall-shear-stress on the space-time dynamics of the lesion.

Numerical Multiphysics for assessing medical intervention

Claude Souprayen[1], Sharad Tripathi[2]

[1] Fluidyn France; [2] Fluidyn India

Quality of numerical simulation of body organs is largely dependent, not only on the availability of computational power or input data but also on the solvers to represent any organ. As it is generally impossible to categorize any organ as solid, liquid or even gas and use corresponding conventional numerical methods, such as Finite Elements, Finite Volumes or again particulate dynamics. More often than not the simulation solvers need to be substantially fine-tuned to the physical properties of the organ.

We have learned to not only tweak the existing solvers for fluids or solids but also make them work together often. Interaction of the body fluids- blood, urine, from skeletal elements, muscles, tendons, skin, etc. require usage of say FEM with FV while each may have changing properties often never seen in everyday simulation of inert matters. Things get still more complex when operating at cellular level.

There is still a lot to research and discover on how to define, things as simple as muscles of organs like eye, ears, respiratory system, simply because of their specialisations. Migration from cells is in itself driven by multiple enzymes and other biochemicals. Thus, isolating one single cause for a pathology is usually not easy. Still more difficult is its correction. We at Fluidyn have worked with researchers to custom made the solvers to respond to a specific problem. Objectives of this paper is to present such a case of collaboration, done many years ago and also the kind of tools that can be made available after required modifications.

As a case example, we'd like to present is of vertigo. A modelling exercise of the movement of crystals, called otolites or otoconies, in a semi-circular canal of internal ear. There are 3 semi-circular and orthogonal to each other canals are present in each year. These canal membranes are filled with a viscous liquid, endolymphe, which detects the rotation on each of the three axes. The sedimentation of free crystals in the fluid in the canal generate loss of equilibrium and vertigo. We'll model the movement of the crystals thru the canals under various forces.

Research Opportunities in EU, France and CNRS

Srini KAVERI
Director, CNRS Bureau, French Embassy, New Delhi

The societal challenges including health issues, demographic change, climate change, need for clean and efficient energy, smart and integrated transport, food security, and the bio-based economy, are no more regional, rather global. Tackling the emerging tasks requires answers that also need to be global and importantly, there is a need for urgent solutions. An efficient international cooperation assisting a link between scientific research and industrial leadership is an absolute necessity to address these tasks.

The European Union proposes several initiatives in this direction through several of its international collaborative research programs. We will also discuss the plans that the French government presents to support and enhance the Indo-French scientific collaborations.

We will discuss the international programs of “Centre National de la Recherche Scientifique” commonly known as CNRS. CNRS is the French National Center for Scientific Research, is a state-funded research organization established in 1939. To its credit, CNRS has and 21 Nobel laureates including that of Jean-Paul Sauvage who won the Nobel this year for his work on ‘molecular machines’ and 12 Fields Medal winners. The organization plays a key role worldwide through International Joint Units and partnerships with more than 60 countries.

In this brief overview, we provide an insight into the tools that facilitate interaction between India and EU with an emphasis on France and CNRS.

Elveflow Microfluidics – high performance pressure & flow control

Sebastian Raja - DSS Imagetech (Indian distributor for Elveflow Microfluidics)

I. Elveflow in a few words

Elveflow provides a comprehensive range of microfluidic instruments that allow automation in many life science experiments and applications.

Our all-in-one solutions include everything you need to perform any microfluidic experiments requiring multiple fluid injection such as drug testing, recirculation or sequence automation in general. Our many configurations and possible options makes it possible for you get a microfluidic setup perfectly fitted to any of your requirements.

II. Our main application packs

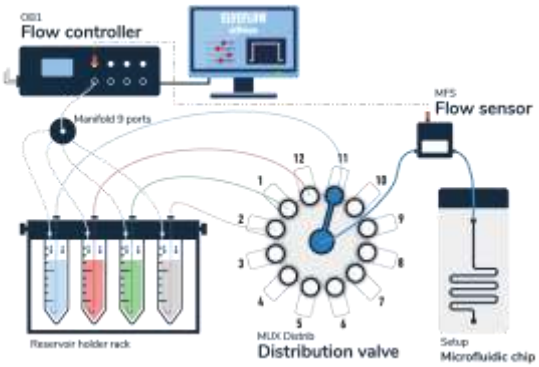

FIG. 1. The Sequential Injection Pack, very useful to switch automatically between different liquids to inject in the same device (3D cell culture / drug screening / sensor testing / calibration)

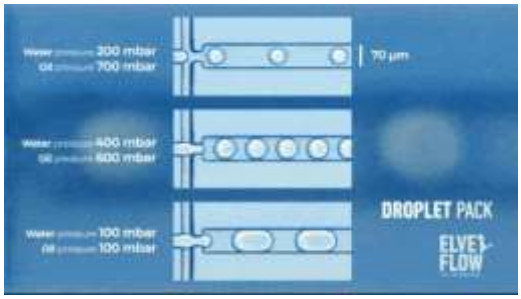

FIG. 2. The Droplet Generation Pack, perfectly suited to make droplets of water in oil from 10 to 80 µm with enhanced user friendliness (hydrogel beads generation / single cell encapsulation / emulsion tests / drop-seq)

FIG. 3. The Lipid Nanoparticle Pack, developed specifically to make LNP generation available to anyone, with large versatility and great performances (vaccine research / human medicine / biotechnologies)

Rapid advances in point-of-care testing through microfluidic technologies, in a post-COVID world

Dhananjaya Dendukuri

Achira Labs

In the post-COVID world, microfluidic technologies are poised to revolutionise point-of-care medical diagnostic testing. They provide multiple benefits such as sample and reagent volume reduction, multi-parameter analysis, automated and rapid workflow and low footprint. In India, small pathology labs, doctor's offices and home testing could benefit from these technologies through instant results for infectious disease testing as well as reduce errors due to degradation or mis-labelling of samples. Further, point-of-care instruments allow for testing in doctor's offices and in many remote settings which are not covered by the current centralized model, thus improving the overall health of our communities. Achira Labs has pioneered the development of an immunoassay platform using the many advantages of microfluidics. The first test panels developed include thyroid and fertility panels and have been validated against gold-standard commercial technologies. The talk will cover advances in microfluidics and point-of-care testing using Achira's technology as a case study.

Dhananjaya Dendukuri is Chief Executive Officer & Co-Founder of Achira Labs, a pioneering point-of-care technology company based out of Bangalore. Dhananjaya returned to India with his passion for engineering and the belief that technology development for underserved markets must be done locally. Starting from his early career experience as a lab scientist and R&D manager (with over 30 publications and 7 issued patents), he now has more than a decade of experience with the fund-raising, commercial, operational and regulatory aspects of building and taking diagnostic technologies to market. He received the National Technology Award for new technologies (biotechnology) in 2016 and MIT Technology Review's prestigious TR35 awards in India for the work that was being done at Achira. Dhananjaya serves on the jury of the Infosys Prize and the X-prize for diagnostics. He received his PhD in Chemical Engineering from MIT, a MASC in Chemical Engineering from the University of Toronto and a B.Tech in Chemical Engineering from the Indian Institute of Technology, Madras.

Lattice Boltzmann Method: A New Paradigm for Multi-Physics Simulations

Vinay Kariwala

SankhyaSutra Labs, Bangalore, India

Abstract:

Use of Computational Fluid Dynamics (CFD) tools allows reduction in effort, cost and time-to-market during the design of products and processes. Lattice Boltzmann Method (LBM) is an emerging technique for high-fidelity multi-physics simulations. With its' roots in kinetic theory of gases, LBM achieves high levels of accuracy and reliability without using explicit turbulence models. LBM scales linearly with available computational power, which makes it an excellent simulation tool for large-scale complex problems. In this talk, we will provide an overview of innovations embedded in SankhyaSutra's LBM technology. We will also demonstrate the potential of LBM using multiple examples taken from various industries including Aerospace & Defense, Automobile and Process Industry.

Biography:

Vinay Kariwala is Head of Business Development at SankhyaSutra Labs in Bangalore, India. Before joining SanskhyaSutra, he worked with ABB India in various roles involving Research, Product Development and Global Technology Management in the areas of Industrial Automation and Digitalization. Vinay was a Professor of Chemical Engineering at Nanyang Technological University in Singapore during 2006-2011. He got his doctoral degree from University of Alberta. He has published 1 book, several book chapters and 100+ publications in journals and conference proceedings.

Author Index